# Chelation-Based Stablization in the Transition-State Structure: Development of Hemilabile Ligand Catalysis

William Collins
Group Meeting (09-12-06)

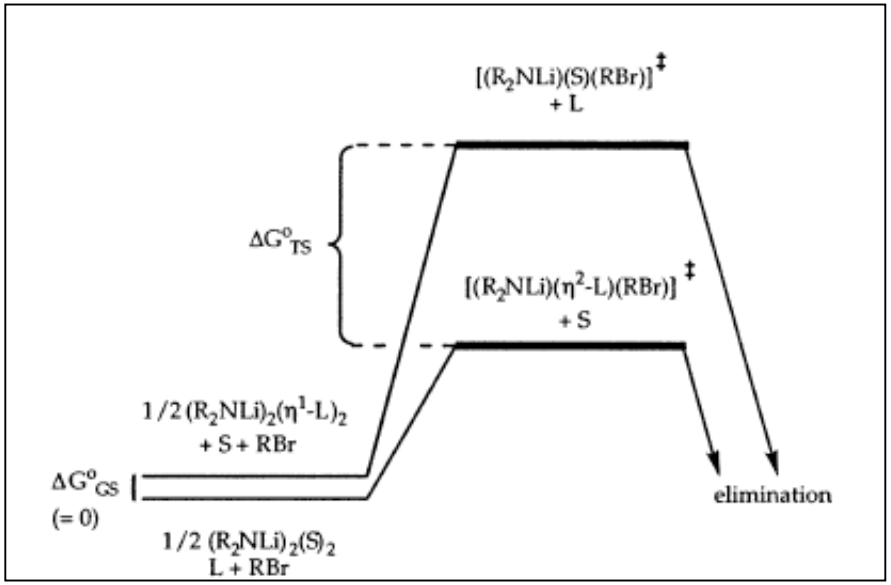


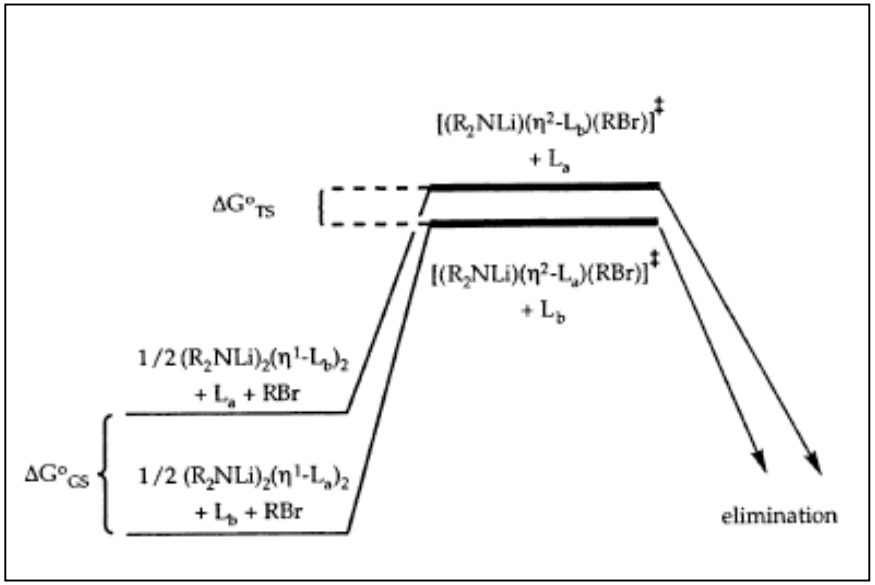


Collum, D. *et. al*. *JACS* **2003**, 125, 15376.

# Outline:

1. Lithium Diisopropylamide Solvation and Solution Structures

2. Chelation-Based Stabilization of the Transition-State Structure in LDA Mediated Dehydrobrominations

3. Catalysis by Hemilabile Ligands in LDA Mediated Enolizations


Collum, D. *Acc. Chem. Res.* **1992**, 25, 448.

# Lithium Diisopropylamide (LDA):

-First discovered by Hamell and Levine (1950)
-Seminal publication: Creger first highlighted the low-nucleophilicity and high kinetic basicity in alpha carboxylic acid deprotonations (1967).
-The crystal structure has been solved many times:

Mulvey (1991):

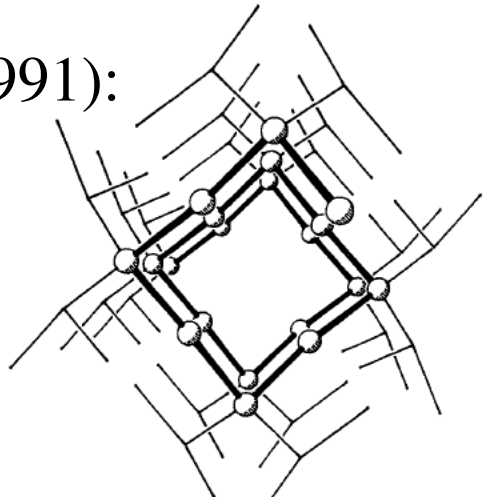

Williard (1993):

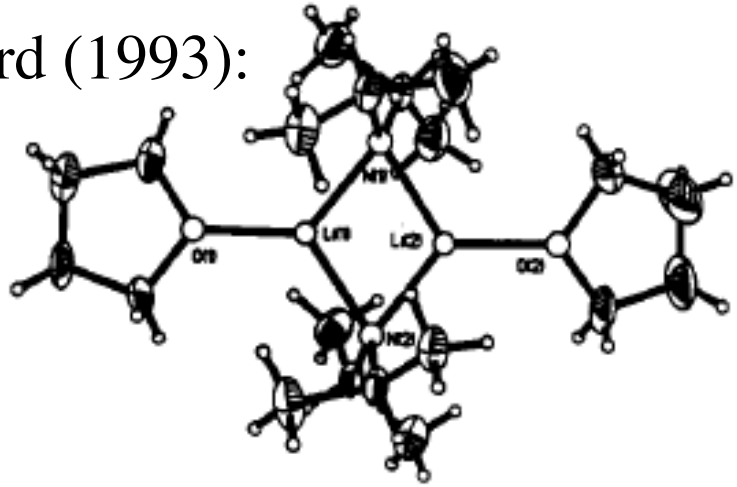

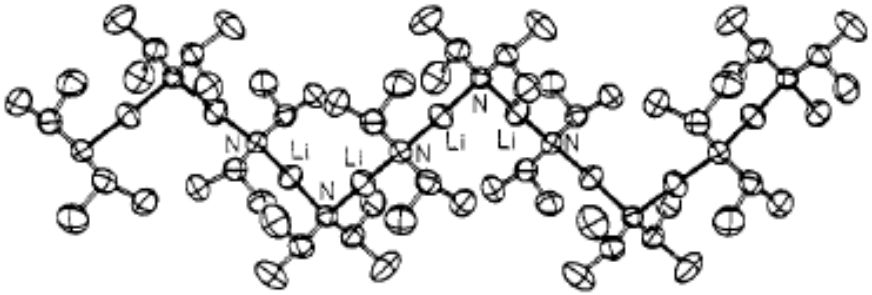


Hammel, M; Levine, R. *JOC*, **1950**, 15, 162.
Creger, P. *JACS*, **1967**, 89, 2500.
Mulvey, R. *et. al JACS*, **1991**, 113, 8187.
Williard, P. *et. al JOC* **1993**, 58, 1.

# Lithium Diisopropylamide Solution Structures:

In solely hydrocarbon solvents LDA exists as a number of oligomers:

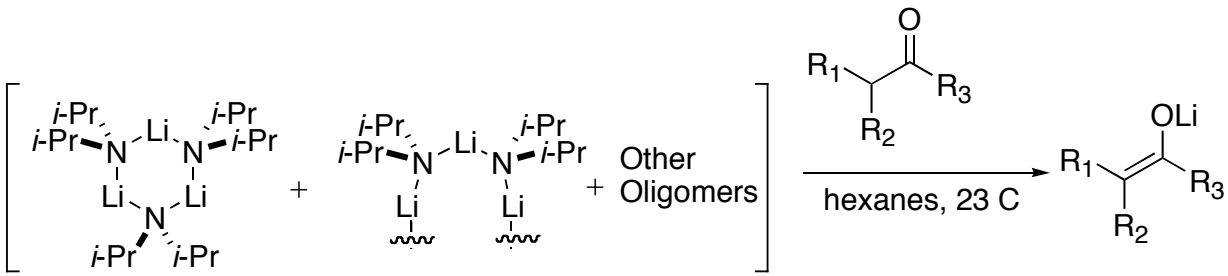


**Table I. Lithium Enolates from Hydrocarbon Solvent**

| entry | substrate | enolate | solvent | % isolated yield |
|---|---|---|---|---|
| 1 | 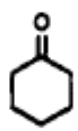 | 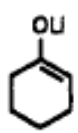 | hexane | 82 (85)[a] |
| 2 |  |  | toluene | 75 |
| 3 | 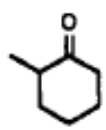 | 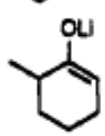 | hexane | 51 (59)[a] |
| 4 | 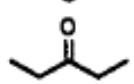 | 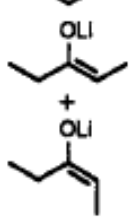 | hexane | 14 |
| 5 | 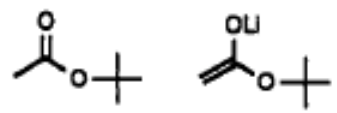 | | hexane | 67 |
| 6 | 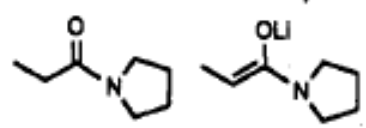 | | hexane | 70 |
| 7 |  | | hexane | 76 |
| 8 | 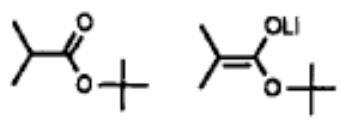 | | hexane | 79 |
| 9 | 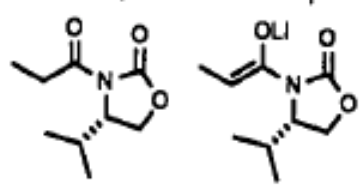 | | hexane | 50 |

Williard, P. *et.al*. *JOC* **1991**, 56, 4435.

# Lithium Diisoproylamide Solution Structures:

Mixtures of 0.1 M [$^{6}$L, $^{15}$N]LDA in 2:1 toluene-pentane with 1.0 equiv of ligand at VT:

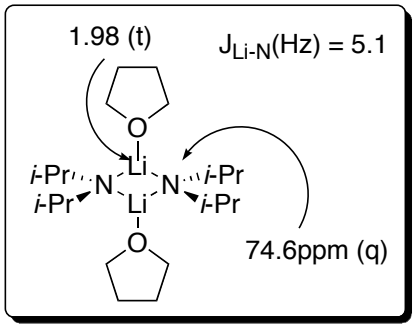


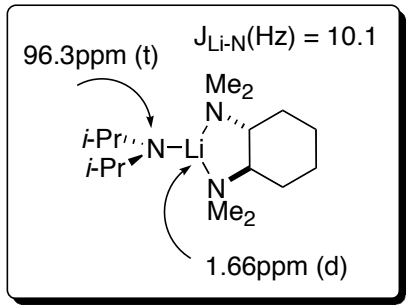


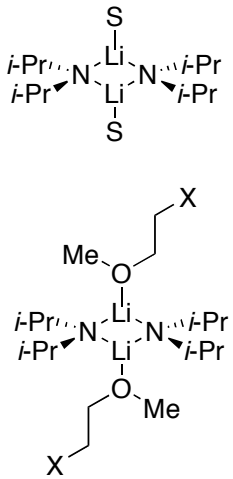

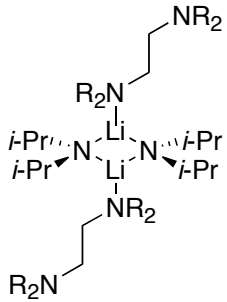

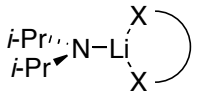

S = $Et_2O$
n-BuOMe
t-BuOMe

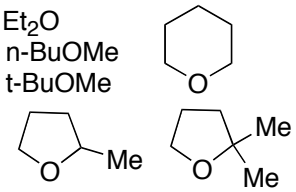

**Ethers:** Cyclic Dimers were the sole product in all cases

X = OMe
$NMe_2$
$NEt_2$

**Amino-Ethers**: Affords disolvated cyclic dimers coordinated through the oxygen (based on LiHMDS)

$NR_2$ = $NMe_2$
$NMe_2$ / N

**Polyamines**:
-TMEDA affords the dimer exclusively.
-The dimethylamino pyrrolidino ethane gives a 25:1 dimer monomer mix.
-Sparteine affords a small amount of monomer w/ substantial amounts of un-solvated oligomers.
-Both trans TMCDA and the isopropyl analog give monomer in prefernce to dimer.

X = Sparteine

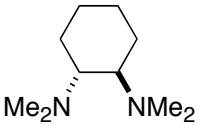

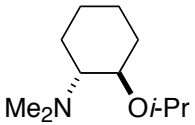

Collum, D. *et. al JACS* **1997**, 119, 5567.

# Relative Ethereal Ligand Binding Constants:

Direct comparison of free and bound ligands through slow exchange is not possible w/ 2(LDA-S). The indirect comparison can be made:

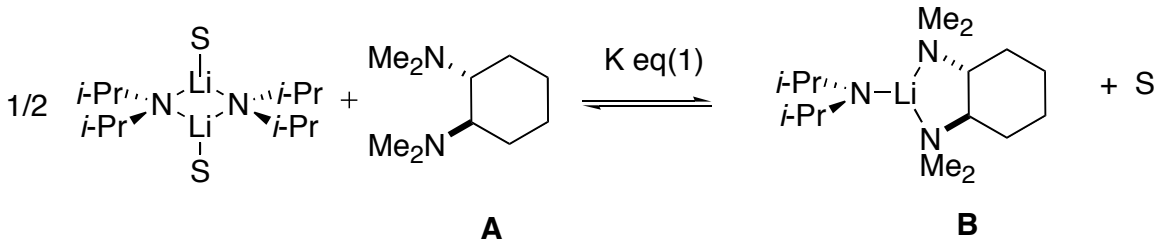


$$\text{Keq(1)} = \frac{[S][B]}{[\text{LDA-S}]^{1/2}[A]}$$

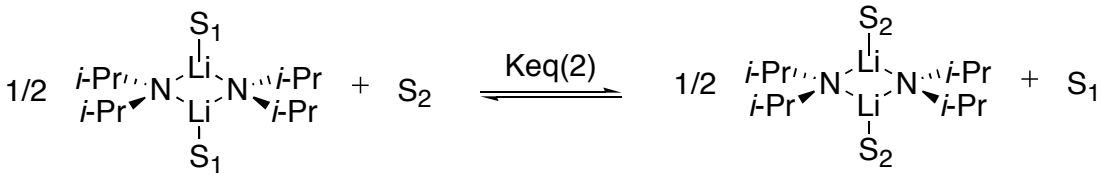


$$\text{Keq(2)} = \frac{(\text{Keq(1) for } S_1)}{(\text{Keq(1) for } S_2)}$$

$$\boxed{\text{Keq(2)} = \frac{([\text{LDA-}S_2]^{1/2}\,[S_1])}{([\text{LDA-}S_1]^{1/2}\,[S_2])}}$$

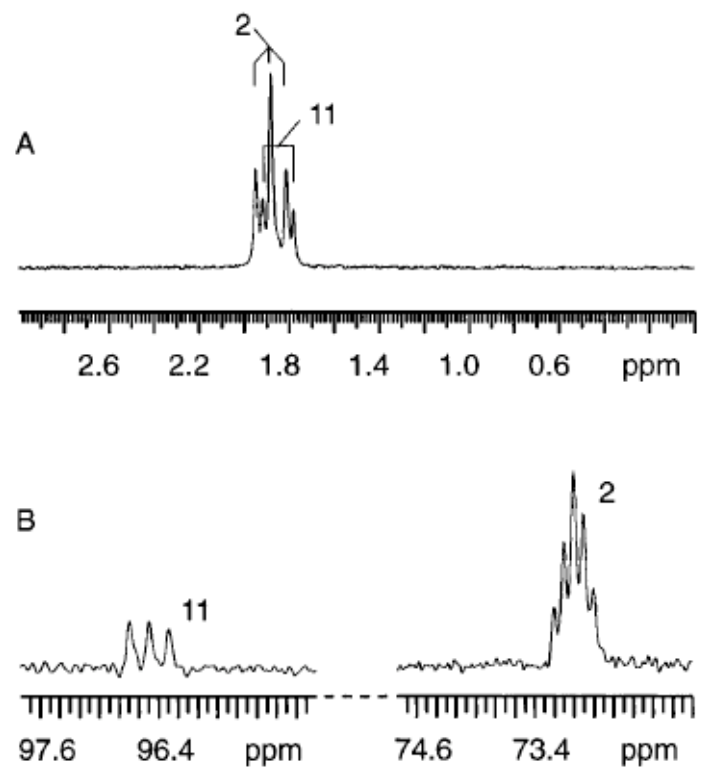


Collum, D. *et. al JACS* **1997**, 119, 5567

# Relative Ethereal Ligand Binding Constants:

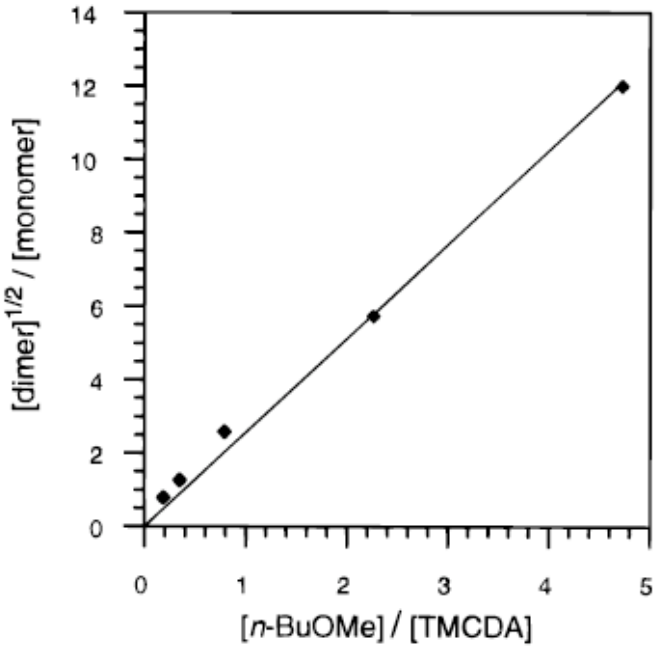


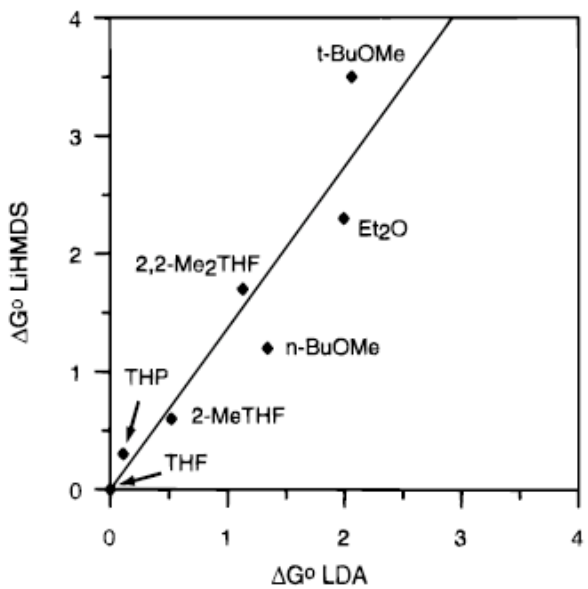


**Table 2.** Binding Constants and Affiliated Free Energies for LDA Dimer Solvation by Ethereal Ligands

| ligand | $K_{eq(1)}$[a] | $K_{eq(2)}$[b] | $\Delta G°$ (kcal/mol)[c] |
|---|---|---|---|
| THF | 0.012 | 1.0 | 0.0 |
| THP | 0.016 | 1.3 | 0.11 |
| 2-MeTHF | 0.045 | 3.8 | 0.52 |
| **I** | 0.124 | 10 | 0.90 |
| **H** (DME) | 0.163 | 14 | 1.0 |
| 2,2-$Me_2$THF | 0.224 | 19 | 1.1 |
| **K** | 0.3 | 25 | 1.2 |
| **J** | 0.34 | 28 | 1.3 |
| *n*-BuOMe | 0.39 | 33 | 1.3 |
| $Et_2O$ | 2.17 | 180 | 2.0 |
| *t*-BuOMe | 2.53 | 210 | 2.0 |

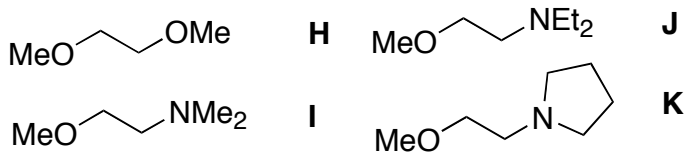


Dimers **H, I, J, K** show binding energies comparable to *n*-BuOMe

Collum, D. *et. al JACS* **1997**, 119, 5567.

# LDA-*n*-BuOMe Mediated Dehydrobrominations:

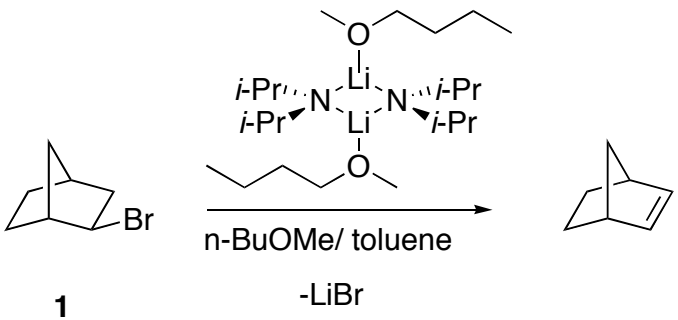


**1**

**$k_H$ / $k_D$ = 1.9 at all [nBuOMe]**

**What is the Stoichiometry of the Transition State Structure?**

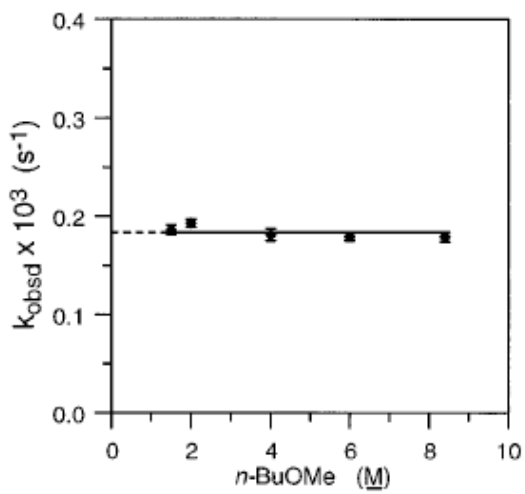


**Figure 1.** Plot of $k_{obsd}$ versus [*n*-BuOMe] in toluene co-solvent for the elimination of **1** (0.004 M) by LDA (0.10 M) at 20 ± 0.1 °C. The curve depicts the result of an unweighted linear least-squares fit to f($x$) = $a$.

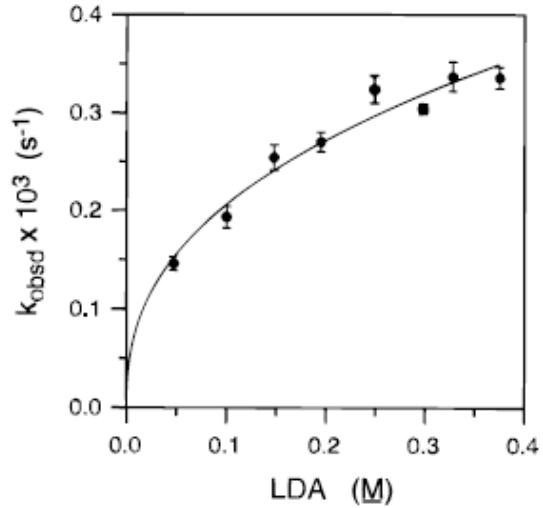


**Figure 2.** Plot of $k_{obsd}$ versus [LDA] for the elimination of **1** (0.004 M) by LDA in *n*-BuOMe (2.0 M) with toluene co-solvent at 20 ± 0.1 °C. The curve depicts the result of an unweighted nonlinear least-squares fit to f($x$) = $ax^b$ ($b$ = 0.40 ± 0.04; see Table 1).

Collum, D. *et. al*, *JACS* **1997**, 119, 5573.

# LDA-*n*-BuOMe Mediated Dehydrobrominations:

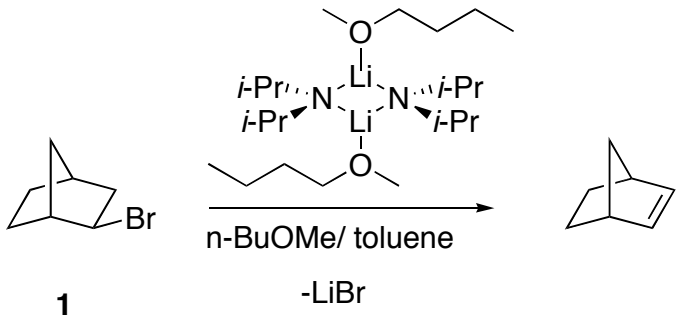


**$k_H$ / $k_D$ = 1.9 at all [nBuOMe]**

**What is the Stoichiometry of the Transition State Structure?**

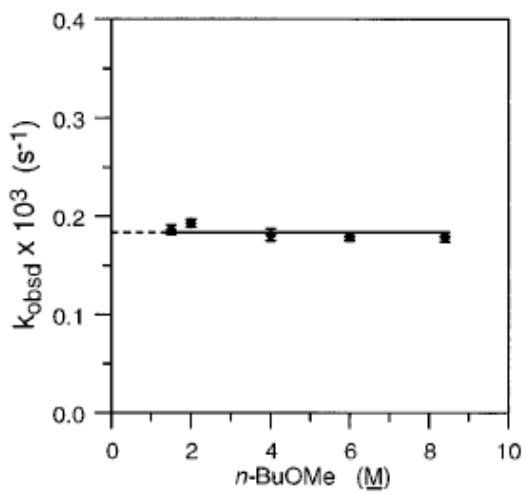


**Figure 1.** Plot of $k_{obsd}$ versus [*n*-BuOMe] in toluene co-solvent for the elimination of **1** (0.004 M) by LDA (0.10 M) at 20 ± 0.1 °C. The curve depicts the result of an unweighted linear least-squares fit to f(*x*) = *a*.

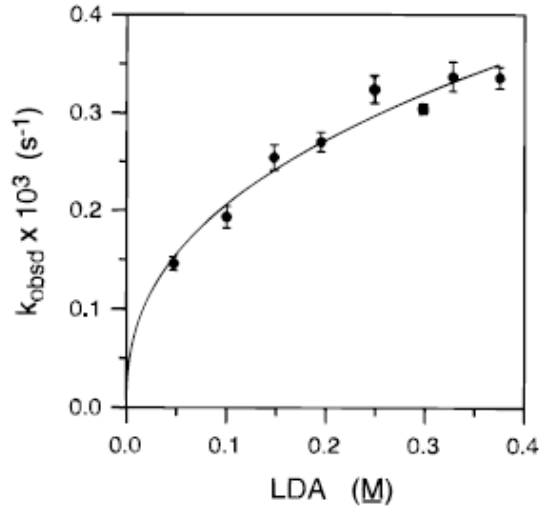


**Figure 2.** Plot of $k_{obsd}$ versus [LDA] for the elimination of **1** (0.004 M) by LDA in *n*-BuOMe (2.0 M) with toluene co-solvent at 20 ± 0.1 °C. The curve depicts the result of an unweighted nonlinear least-squares fit to $f(x) = ax^b$ ($b = 0.40 \pm 0.04$; see Table 1).

**Rate Equation:**

$$-d[\mathbf{1}] / dt = k_{obsd}[\mathbf{1}]$$

such that $k_{obsd} = k'[LDA]^{1/2}$ [S]

**Potential Mechanism:**

$$1/2\ (i\text{-}Pr_2)NLi\text{-}S)_2 \rightleftharpoons i\text{-}Pr_2NLi\text{-}S$$

$$i\text{-}Pr_2NLi\text{-}S + \mathbf{1} \longrightarrow \text{norbornene}$$

Collum, D. *et. al*, *JACS* **1997**, 119, 5573.

# LDA-DME Mediated Dehydrobrominations:

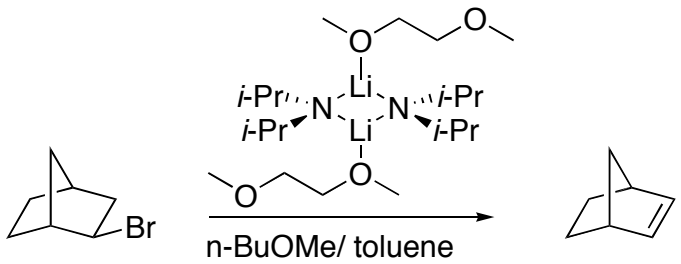


**1**

**$k_H$ / $k_D$ = 2.8 at all [DME]**

**LDA order:** 0.55 +/- 0.02
**DME order:** 0

**Rate Equation:**

$$-d[\mathbf{1}] / dt = k_{obsd}[\mathbf{1}]$$

such that $k_{obsd} = k'[LDA]^{1/2}$ [S]

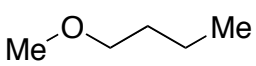


**(1)**

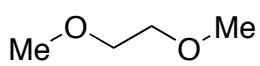


**(50)**

Collum, D. *et. al, JACS* **1997**, 119, 5573.

# LDA-DME Mediated Dehydrobrominations:

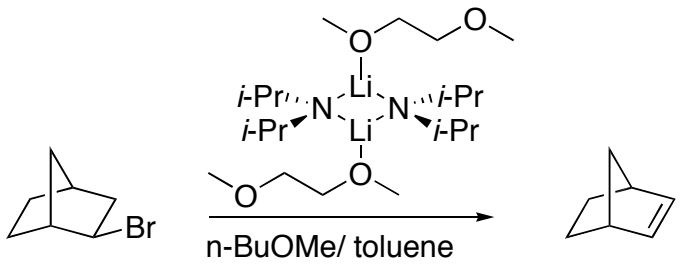


**1**

**$k_H$ / $k_D$ = 2.8 at all [DME]**

**LDA order:** 0.55 +/- 0.02
**DME order:** 0

**Rate Equation:**

$$-d[\mathbf{1}] / dt = k_{obsd}[\mathbf{1}]$$

such that $k_{obsd} = k'[LDA]^{1/2}$ [S]


**(1)** **(50)**

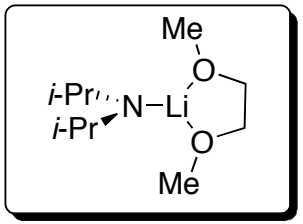


Collum, D. *et. al, JACS* **1997**, 119, 5573.

# LDA-Lewis Base Mediated Dehydrobrominations:

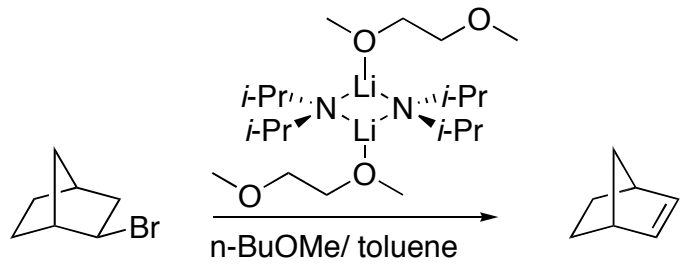


$k_H / k_D$ **= 2.8 at all [DME]**

**LDA order:** 0.55 +/- 0.02
**DME order:** 0

**Rate Equation:**

$$-d[\mathbf{1}] / dt = k_{obsd}[\mathbf{1}]$$

such that $k_{obsd} = k'[LDA]^{1/2}[S]$

## Relative Rates of Dehydrobromination:

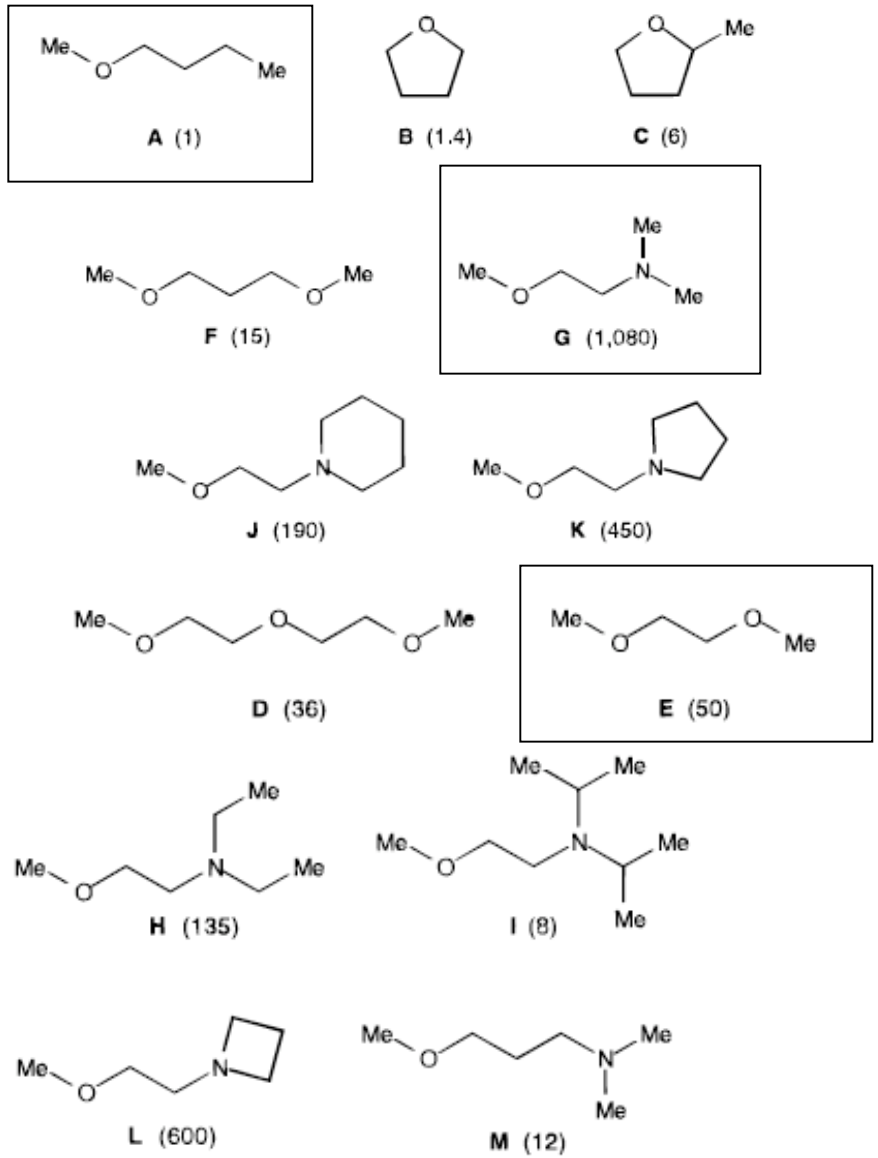


Collum, D. *et. al, JACS* **1997**, 119, 5573.

# Avoiding the "Universal Ground State" Approximation

The interpretation of the relative rates hinges upon the assumption that the cyclic-dimer lewis base complexes are related by thermoneutral ligand substitution.

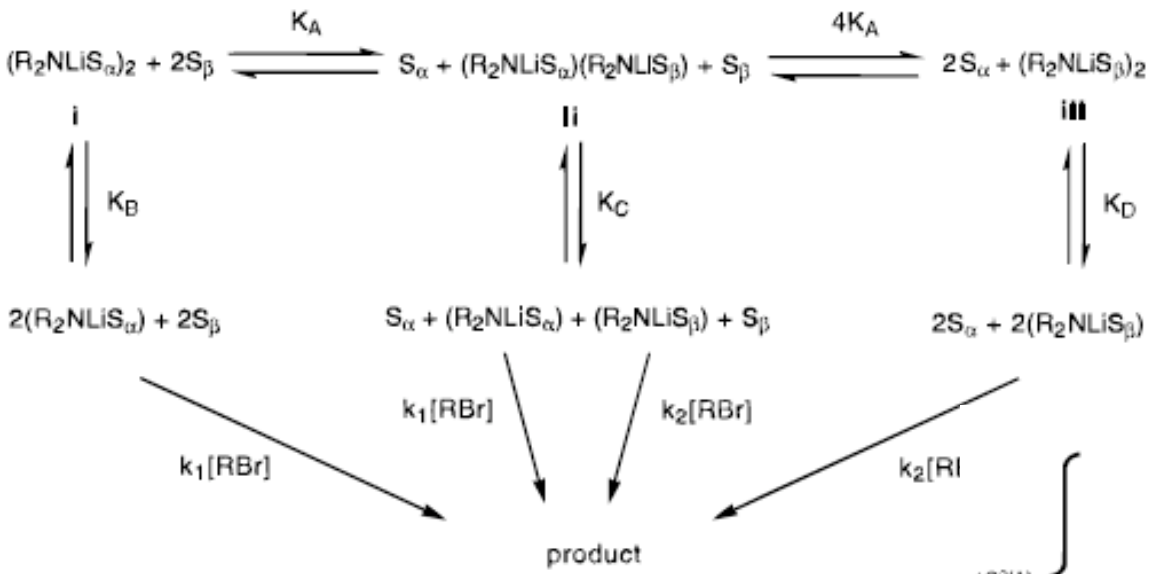


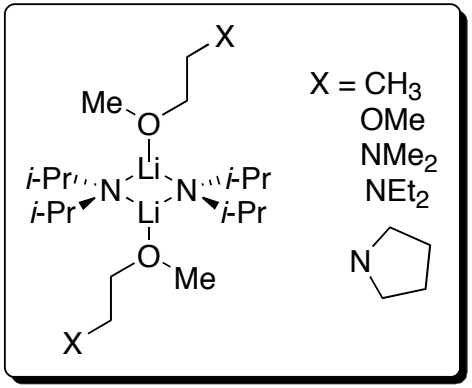


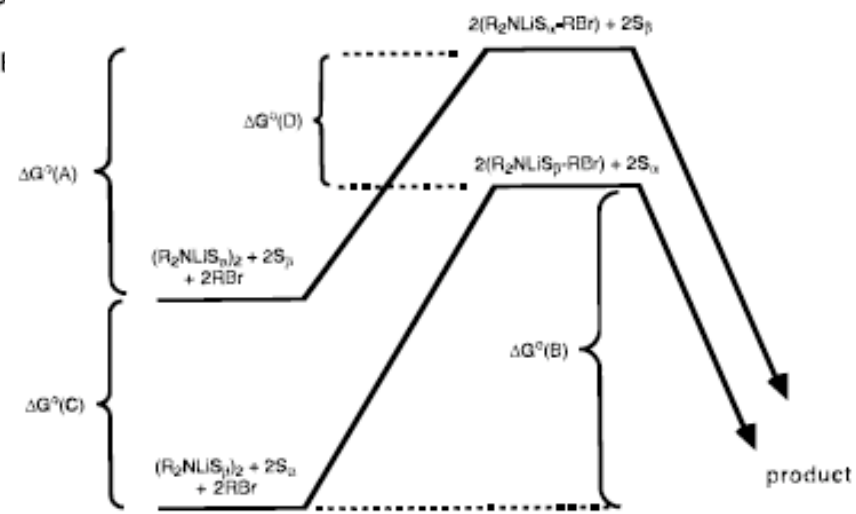


Collum, D. *et. al, JACS* **1997**, 119, 5573

# Kinetics of Elimination Provide Thermodynamics of Solvation

$$k_{obsd} = \left\{ k_1 K_B^{1/2} + k_2 K_D^{1/2} \left( 2K_A \frac{[S_\beta]}{[S_\alpha]} \right) \right\} \times \left\{ \frac{A_T}{1 + K_A \frac{[S_\beta]}{[S_\alpha]} + \left( 2K_A \frac{[S_\beta]}{[S_\alpha]} \right)^2} \right\}^{1/2} \quad (8)$$

$$k_{obsd} = \left\{ k_1 K_B^{1/2} + k_2 K_D^{1/2} \left( 2K_A \frac{[X_2]}{[1 - X_2]} \right) \right\} \times \left\{ \frac{A_T}{1 + K_A \frac{[X_2]}{[1 - X_2]} + \left( 2K_A \frac{[X_2]}{[1 - X_2]} \right)^2} \right\}^{1/2} \quad (9)$$

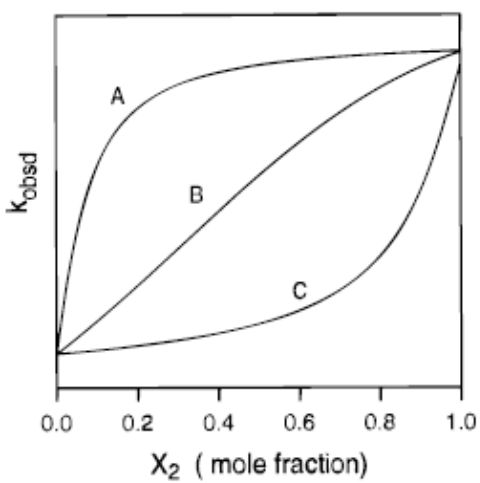


**Figure 5.** Predicted rate constants ($k_{obsd}$) vs mole fraction ($X_2$) of solvent $S_\beta$ in co-solvent $S_\alpha$ according to eq 9. Assumptions: ($k_{obsd}$ in neat $S_\beta$)/($k_{obsd}$ in neat $S_\alpha$) = 10; $K_A$ = 10 (curve A), 1.0 (curve B), and 0.1 (curve C).

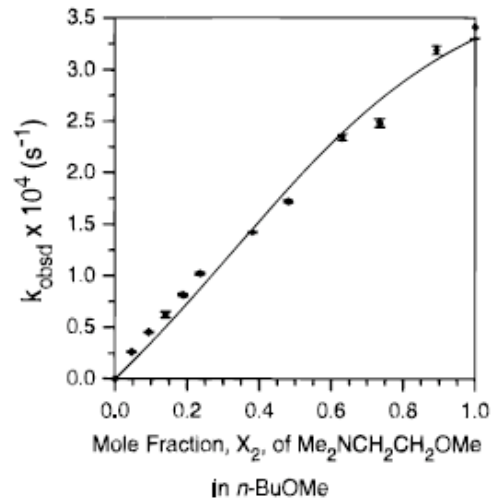


**Figure 6.** Observed rate constants for dehydrobromination of **1** by LDA vs mole fraction of $Me_2NCH_2CH_2OMe$ ($X_2$) in *n*-BuOMe under the following conditions: −20 °C; [LDA] = 0.10 M; [**1**] =0.004 M. The curve corresponds to a nonlinear least-squares fit to eq 10, affording $K_A$ = 1.02 ± 0.09 and $k_2K_D$ = 1.05 ± 0.02 × $10^{-2}$.

**$K_A(S_B/S_a)$ Relative to *n*-BuOMe**

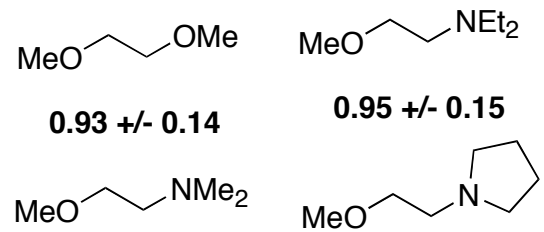


**0.93 +/- 0.14** **0.95 +/- 0.15**

**1.02 +/- 0.09** **0.81 +/- 0.11**

**$\Delta G^O$(C) <0.05 KCal/mol**

Collum, D. *et. al*, *JACS* **1997**, 119, 5573

# Implications of Equivalent Binding Constants:

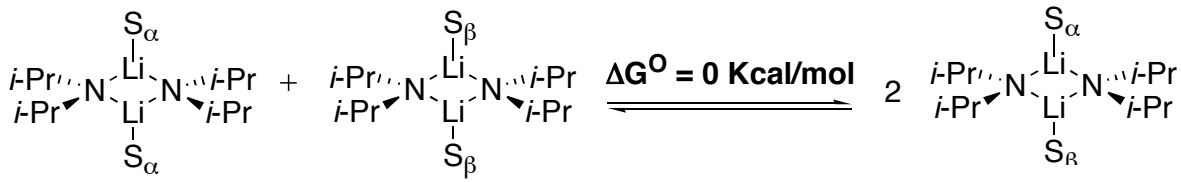


## Potential TS Structure:

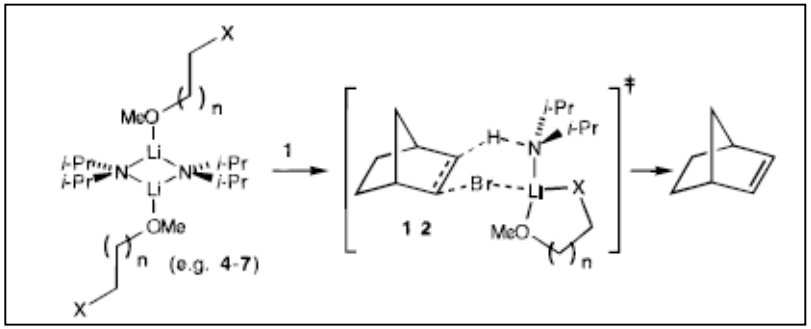


F (15)

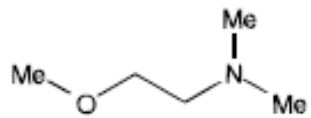

G (1,080)

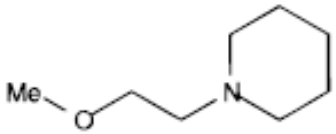

J (190)

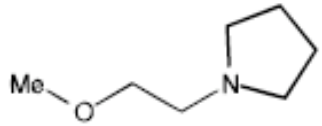

K (450)

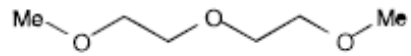

D (36)

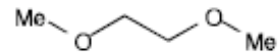

E (50)

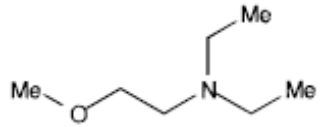

H (135)

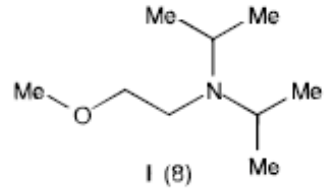

I (8)

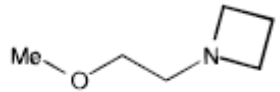

L (600)

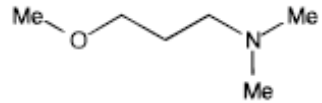

M (12)

Collum, D. *et. al, JACS* **1997**, 119, 5573

# Implications of Equivalent Binding Constants:

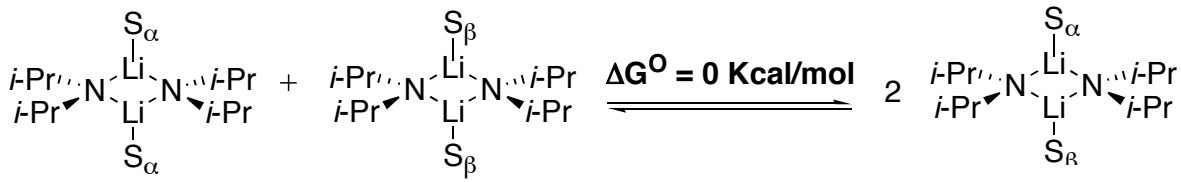


## Potential TS Structure:

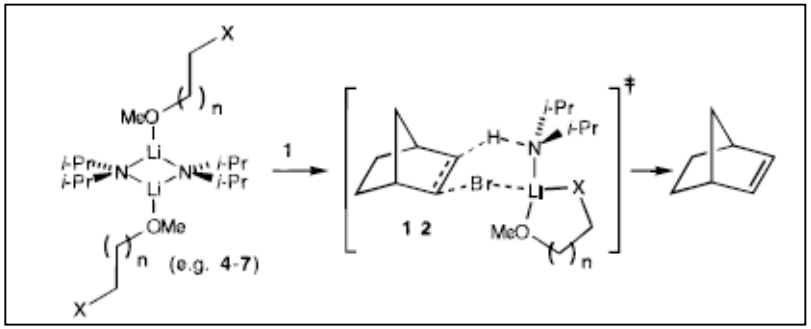


**F** (15)

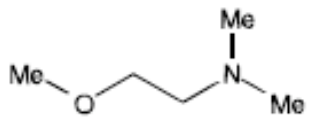

**G** (1,080)

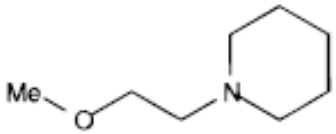

**J** (190)

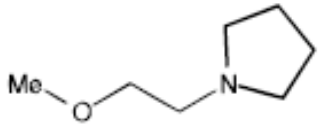

**K** (450)

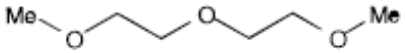

**D** (36)

**E** (50)

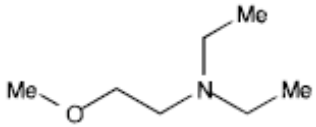

**H** (135)

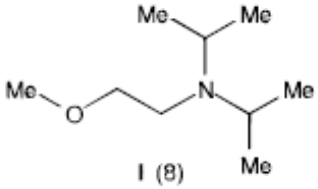

**I** (8)

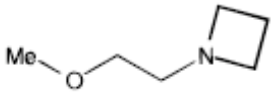

**L** (600)

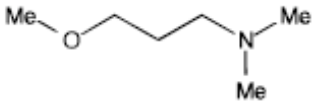

**M** (12)

A) Chelate ring size is critical.
B) TS structure stabilization correlates inversely w/ increasing bulk on pendant ligand.
C) The 20-Fold rate increase of **G** over **E** implies higher azaphilicity than oxophilicity at the TS

Collum, D. *et. al*, *JACS* **1997**, 119, 5573

# Thermochemical analysis of Hemilibility

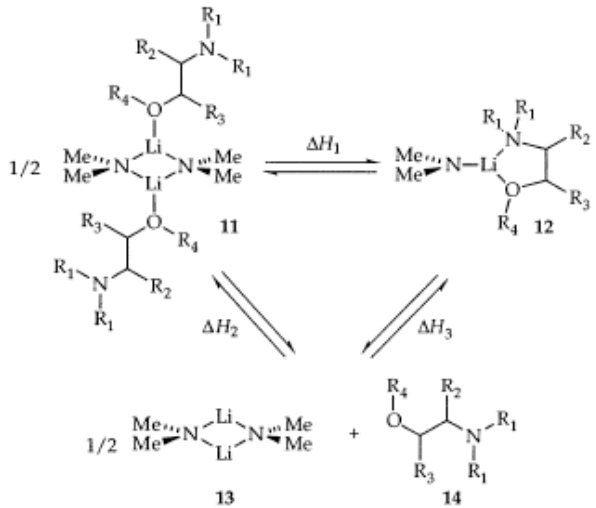


*Table 2.* Calculated Enthalpies (kcal/mol) of Monomer Aggregation ($\Delta H_1$), Dimer Solvation ($\Delta H_2$), and Monomer Solvation ($\Delta H_3$) for $Me_2NLi$ Coordinated to Ligands of General Structure $MeOCH_2CH_2NR_2$[a]

| ligand | $H_{f(Ligand)}$ | $\Delta H_1$ | $\Delta H_2$ | $\Delta H_3$ |
|---|---|---|---|---|
| **A** | −44.1 | 10.4 | −6.8 | 3.6 |
| **B** | −51.0 | 11.3 | −7.1 | 4.2 |
| **C** | −50.3 | 16.0 | −6.2 | 9.8 |
| **D** | −17.9 | 9.0 | −6.7 | 2.3 |
| **E** | −37.9 | 10.0 | −6.8 | 3.2 |
| **F** | −54.6 | 12.4 | −6.8 | 5.6 |
| **G** | −55.9 | 13.6 | −6.8 | 6.8 |
| av dev[b] | – | 2.4 | 0.3 | 2.6 |

[a] The heats of formation (kcal/mol) of ligands **A**−**G** in their most stable conformations are represented by $\Delta H_{f(Ligand)}$. $(Me_2NLi)_2$ = −60.5 kcal/mol. [b] Av dev = average deviation.

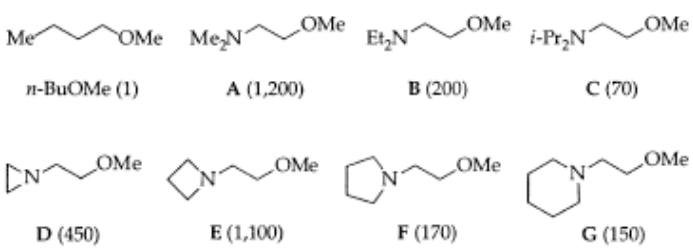


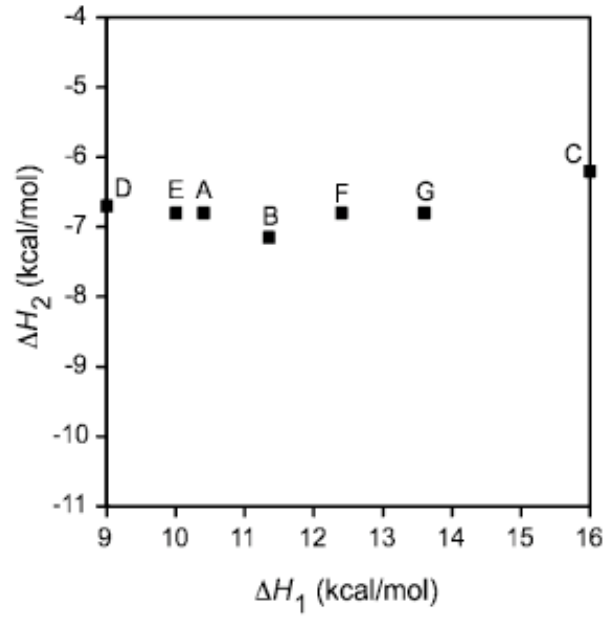


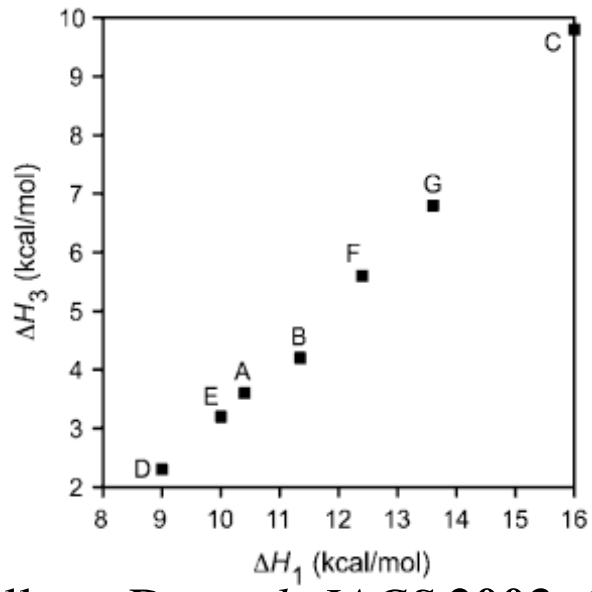


Collum, D. *et.al*. *JACS* **2003**, 125, 15376

# Hemilabile Ligands:

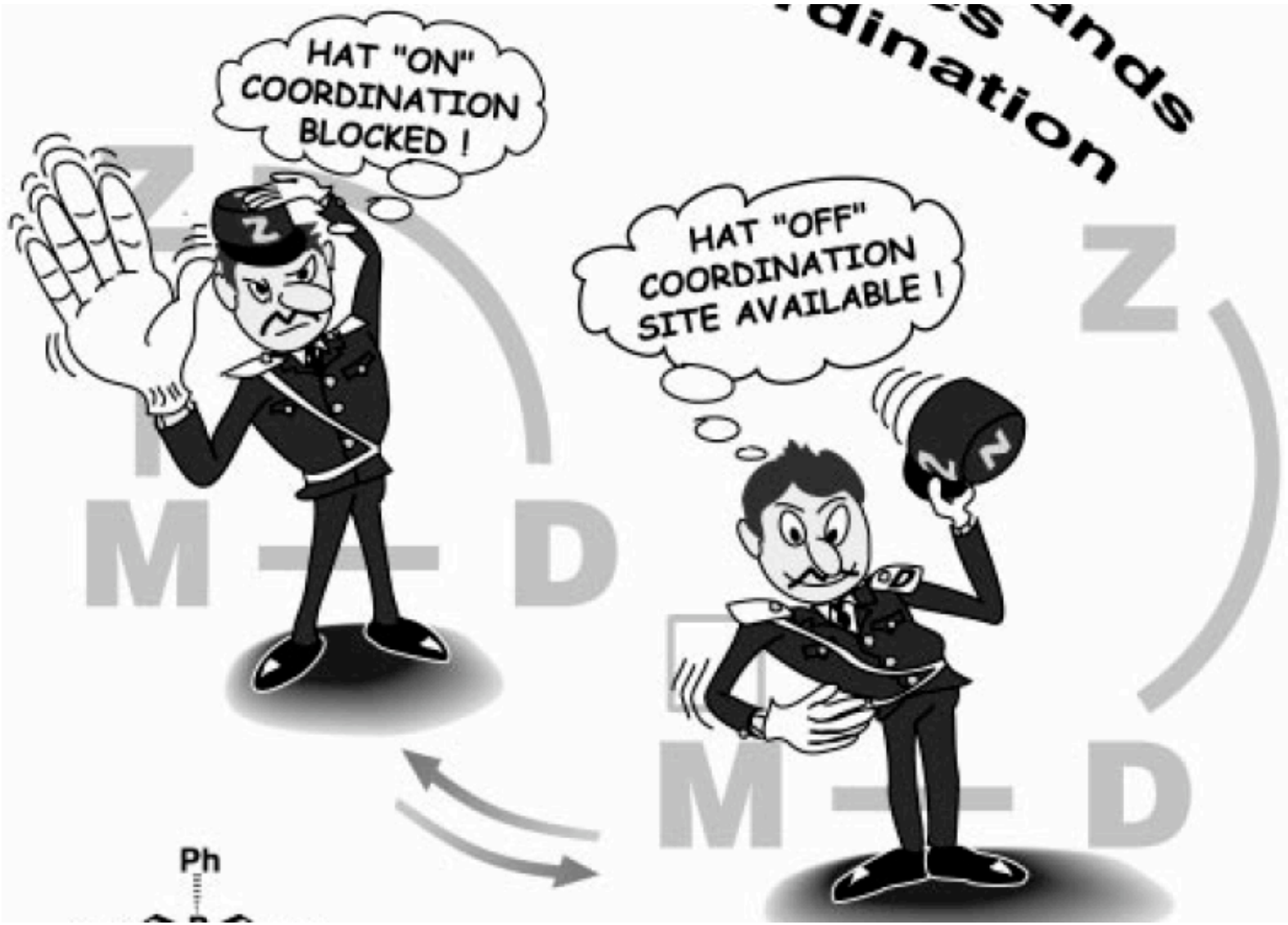


Braunstein, P. *et. al. Angew. Chem. Int. Ed.* **2001**, 40, 680

# Hemilabile Ligands:

By using a ligand $\eta^1$ coordinated in the reactant and $\eta^2$ in the TS structure achieves 2 goals:

1) Maximizes the benefits of chelation by eliminating counterproductive stabilization of the reactant

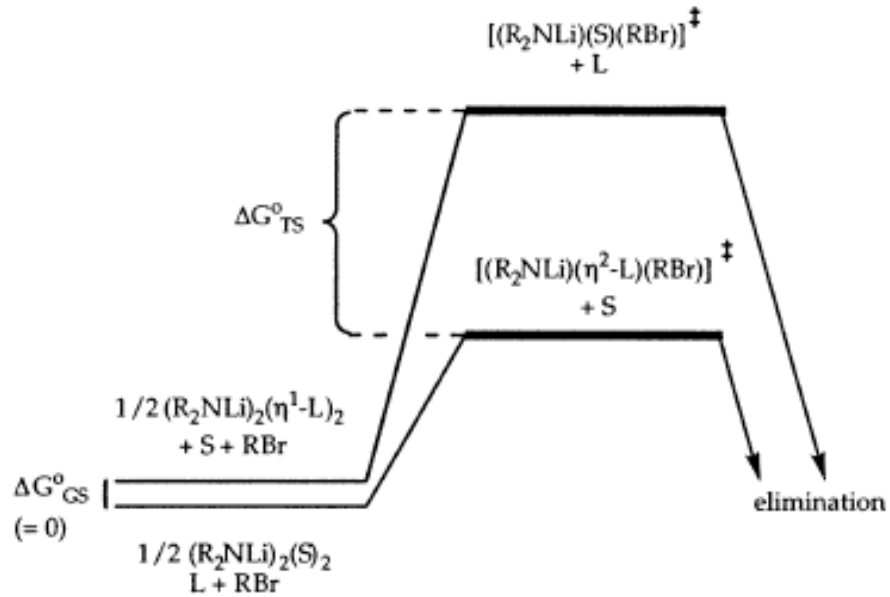


2) The absence of chelation in the ground state allows a direct assessment of how a ligand's structural features and chain length influence chelation at the TS structure.

Collum, D. *et.al*. *JACS* **2003**, 125, 15376.

# Lewis Base Catalyzed Organolithium Reactions:

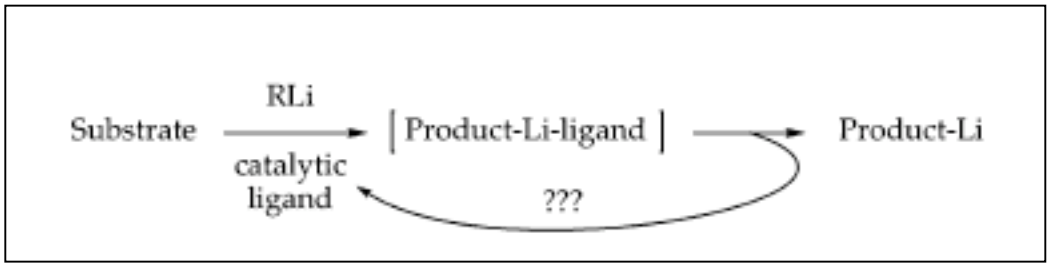


## Successful Examples:

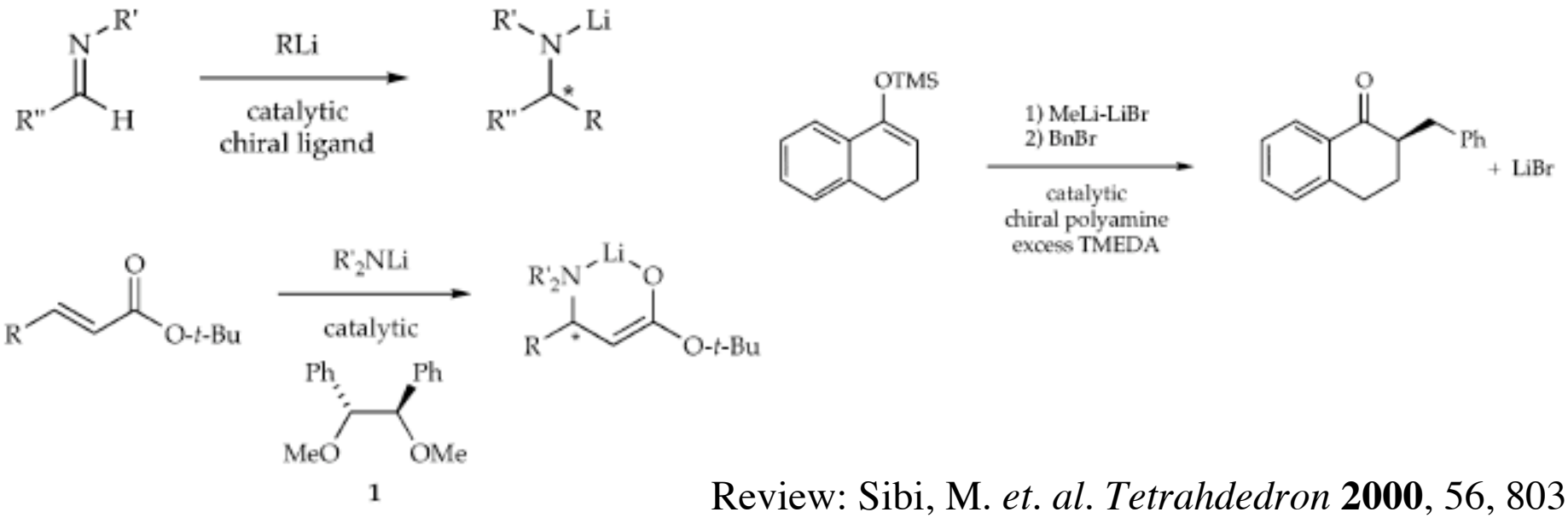


Review: Sibi, M. *et. al. Tetrahdedron* **2000**, 56, 8033
Denmark, S. *et. al. J. Chem. Soc.* **1996**, 999.
Collum, D. *et.al. JACS* **2006**, 128, 10326.
Tomioka, K *et. al JACS* **2003**, 125, 2886.
Koga, K *et. al. JACS* **1994**, 116, 8829.

# General Kinetics of Enolization:

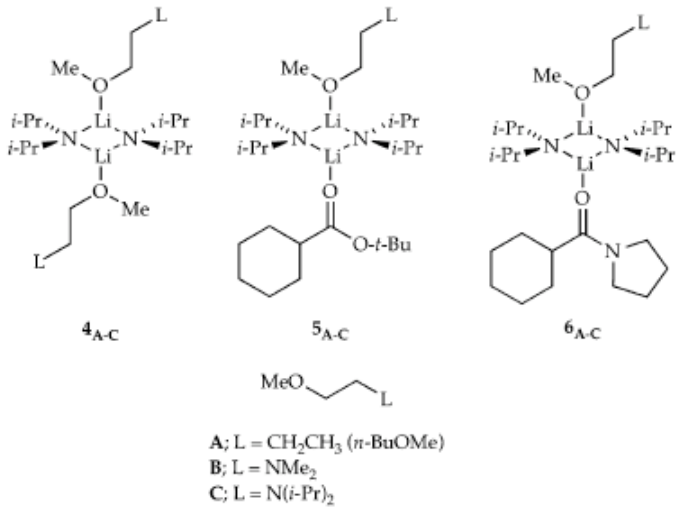


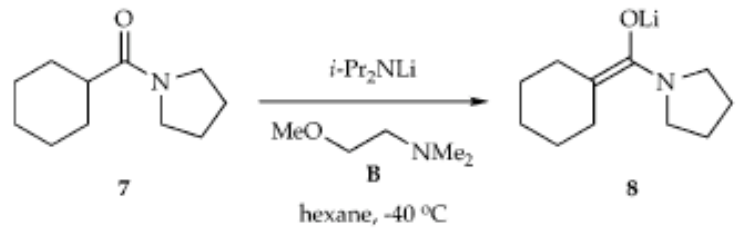


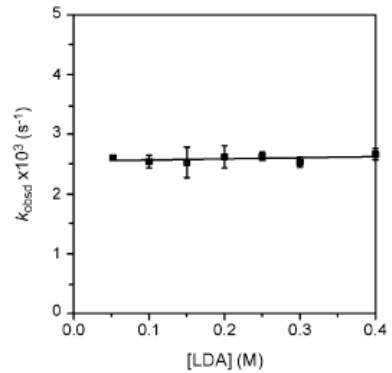


***Figure 1.*** Plot of $k_{obsd}$ vs [LDA] in *n*-BuOMe (0.5 M) and hexane cosolvent for the enolization of **7** (0.004 M) at 0 °C. The curve depicts an unweighted least-squares fit to $k_{obsd} = k\,[\mathrm{LDA}] + k'$ ($k = (2 \pm 2) \times 10^{-4}$, $k' = (2.5 \pm 0.1) \times 10^{-3}$).

***Table 2.*** Relative Rate Constants for the LDA-Mediated Enolization of Ester **2** ($k_{rel}1$, eq 6) and Carboxamide **7** ($k_{rel}2$, eq 7) in the Presence of Hemilabile Ligands

| ligand[a] | $k_{rel}1$[b] | $k_{rel}2$[c] |
|---|---|---|
| **A**; *n*-BuOMe | 1 | 1 |
| **B**; $MeOCH_2CH_2NMe_2$ | 10,000 | 30 |
| **C**; $MeOCH_2CH_2N(i\text{-}Pr)_2$ | 10 | 3 |

[a] [Ligand] = 0.5 M. [b] Measured at −78 °C. [c] Measured at −30 °C.

***Table 3.*** Summary of Rate Studies for the LDA-Mediated Enolization of Carboxamide **7** (eq 7)

| entry | temp (°C) | ligand | LDA[a] order | ligand order | $k_H/k_D$ |
|---|---|---|---|---|---|
| 1 | 0 | A | 0 | 0 | 6.2 ± 0.7 |
| 2 | −40 | B | 0 | 0 | 7.5 ± 0.5 |
| 3 | −30 | C | 0 | 0 | 6.3 ± 0.3 |

[a] [Ligand] = 0.5 M.

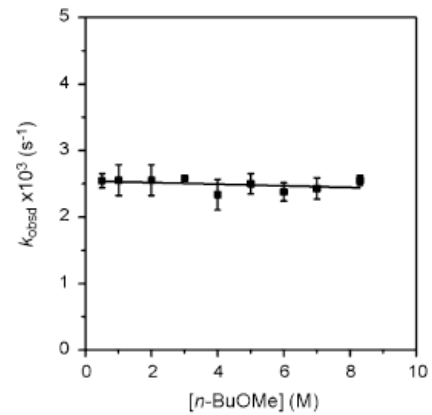


***Figure 2.*** Plot of $k_{obsd}$ vs [*n*-BuOMe] in hexane cosolvent for the enolization of **7** (0.004 M) by LDA (0.10 M) at 0 °C. The curve depicts an unweighted least-squares fit to $k_{obsd} = k\,[n\text{-BuOMe}] + k'$ ($k = (-1 \pm 1) \times 10^{-5}$, $k' = (2.5 \pm 0.1) \times 10^{-3}$).

Collum, D. *et.al*. *JACS* **2006**, 128, 10326.

# General Kinetics of Enolization

$$-d[6]/dt = k'[6]$$

$$(i\text{-}Pr_2NLi)_2(\text{ligand})(7) \rightarrow \text{enolate}$$

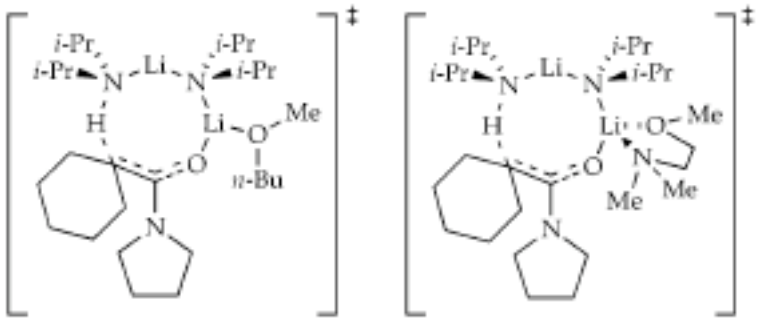


$9_A$




$10_B$

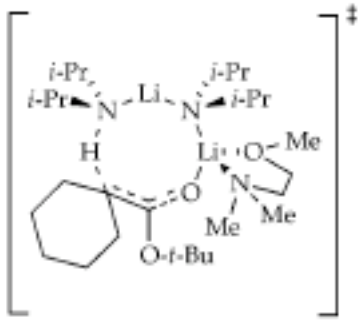


$11_B$

Rate studies of ester with ligand **C**: enolization rates are independent of [**C**] or [**LDA**]

Collum, D. *et.al*. *JACS* **2006**, 128, 10326.

# Mixed Aggregation and Autoinhibition

Sources of Autoinhibition:

1) The formation of unreactive heteroaggregates
2) Strong binding of the ester or catalyst to homo / heteroaggregated enolate

Important points to consider:

1) Mixed aggregate equilibria shift to maximize the number of chelated lithiums
2) The existence of chelation is dictated by congestion within the aggregates
3) The enolate is less sterically demanding than the *i*-Pr2NLi moiety

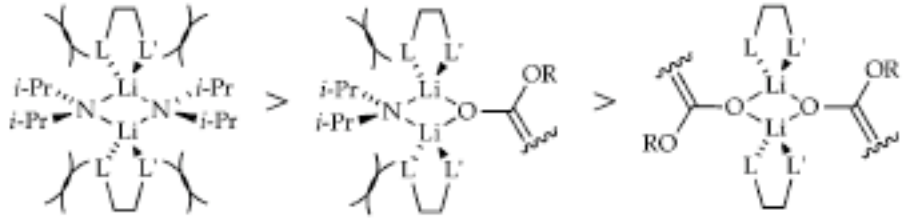


Collum, D. *et.al*. *JACS* **2006**, 128, 10326.

# Enolization of Ester w/ LDA-nBuOMe

Enolization of **2** by 1.0 equiv of LDA at -25 C in 1.0 M nBuOMe / hexanes: rxn stalls at 50% conversion

-Still large excess of nBuOMe, IR shows >95% of ester still uncomplexed

Spectroscopic analysis on rxns <50% conversion:

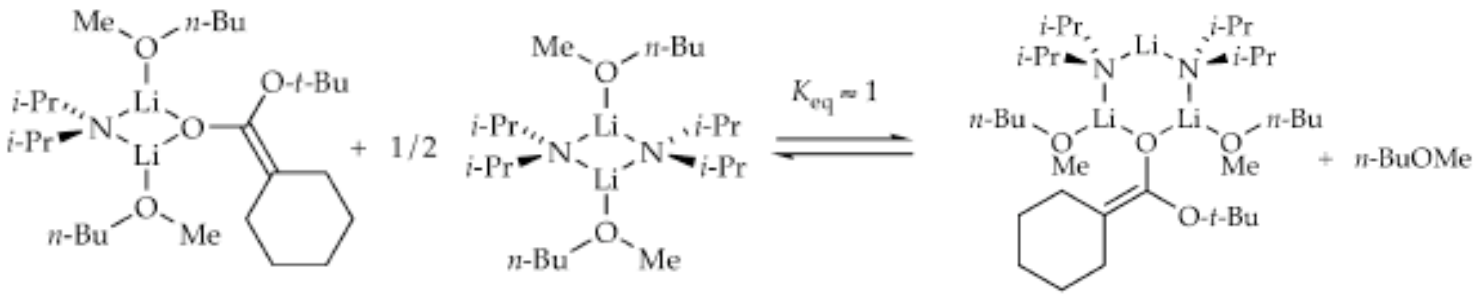


Rxn at 50% conversion:

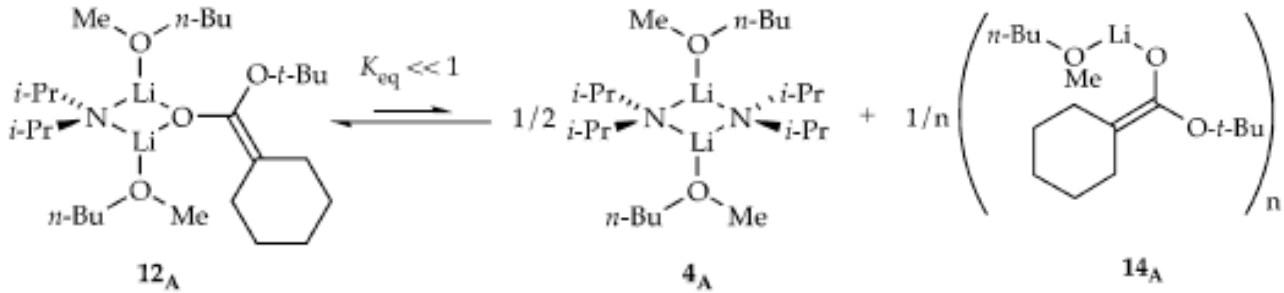


Collum, D. *et.al*. *JACS* **2006**, 128, 10326.

# Enolization of Ester w/LDA-LB

Enolization of **2** by 1.0 equiv of LDA at -78 C, (11.0 equiv aminoether) in hexanes: rxn stalls at 50% conversion

-Proceeds to full conversion after 2nd equiv of LDA

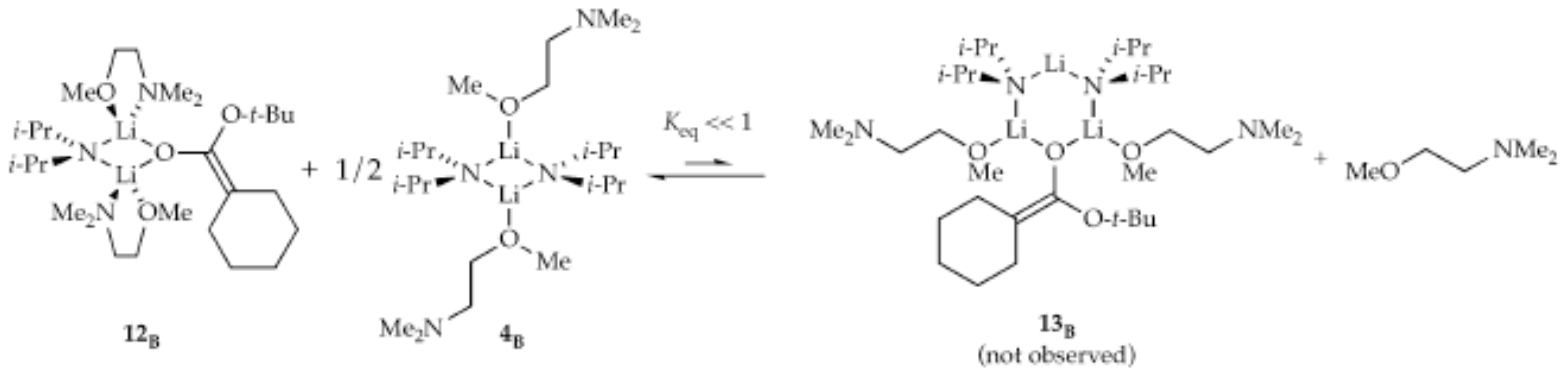


Low temp NMR experiment (-125 C):

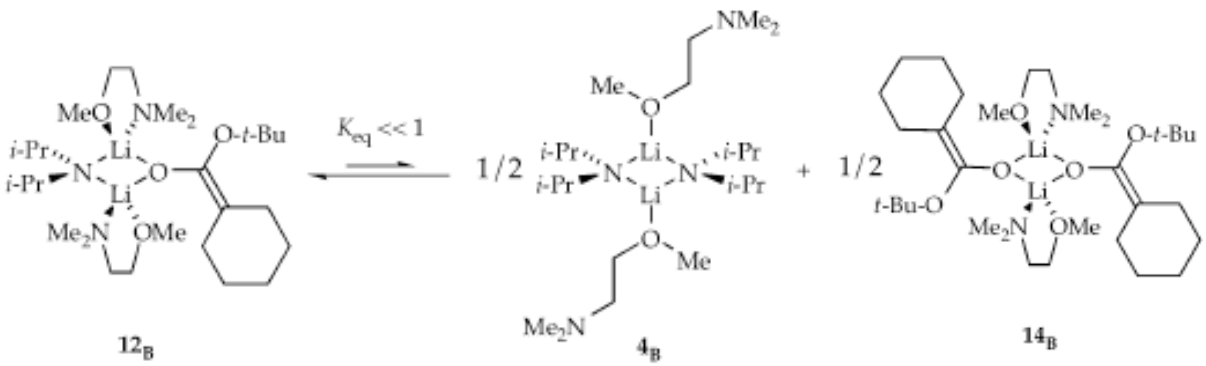


Collum, D. *et.al*. *JACS* **2006**, 128, 10326

# Enolization of Ester w/LDA-LB

<50% conversion:

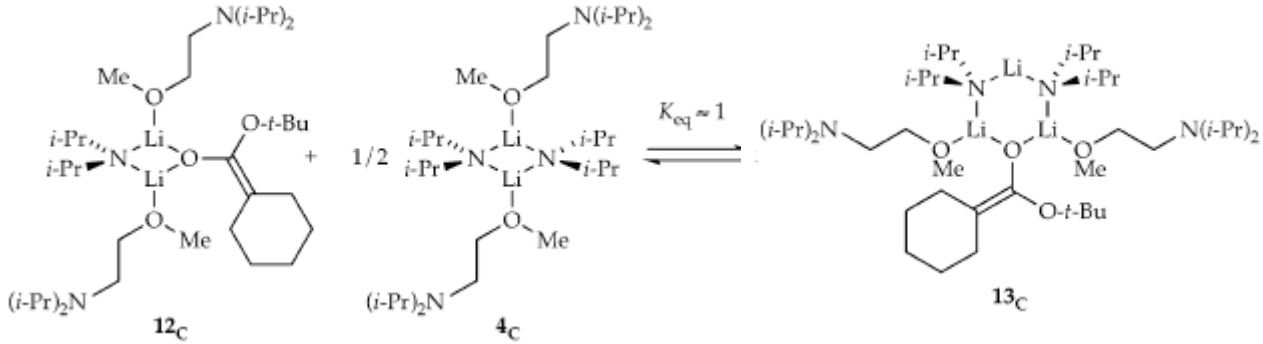


Similar to nBuOMe except: 1) Enolizations taken to 50% conversion contain considerable amount of 4c dimer and lithium enolate 14c
2) Autoinhibition is considerably less pronounced for this enolization

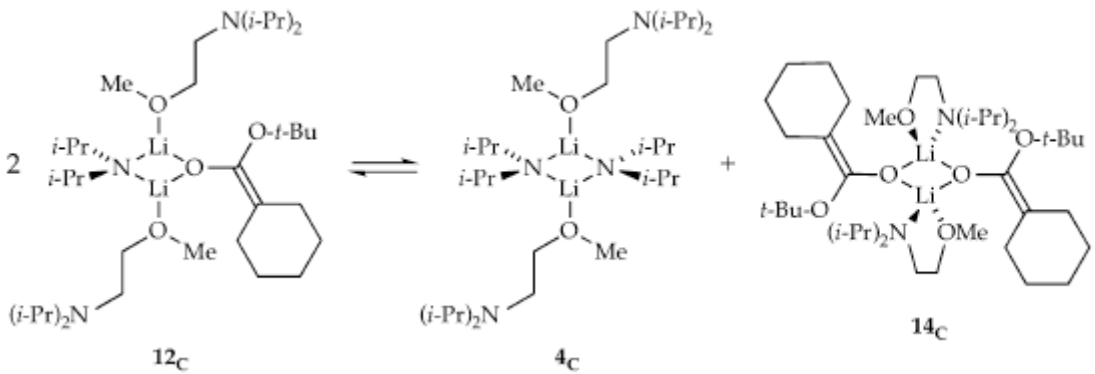


Collum, D. *et.al*. *JACS* **2006**, 128, 10326

# Summary of Enolization:

A) Enolizations of the ester by 1.0 equiv. of LDA stall at 50% Conversion due to mixed aggregates

B) Amino-ether **B** forms stable chelates of mixed dimer **12B** relative to mixed trimer as well as the homoaggregates.

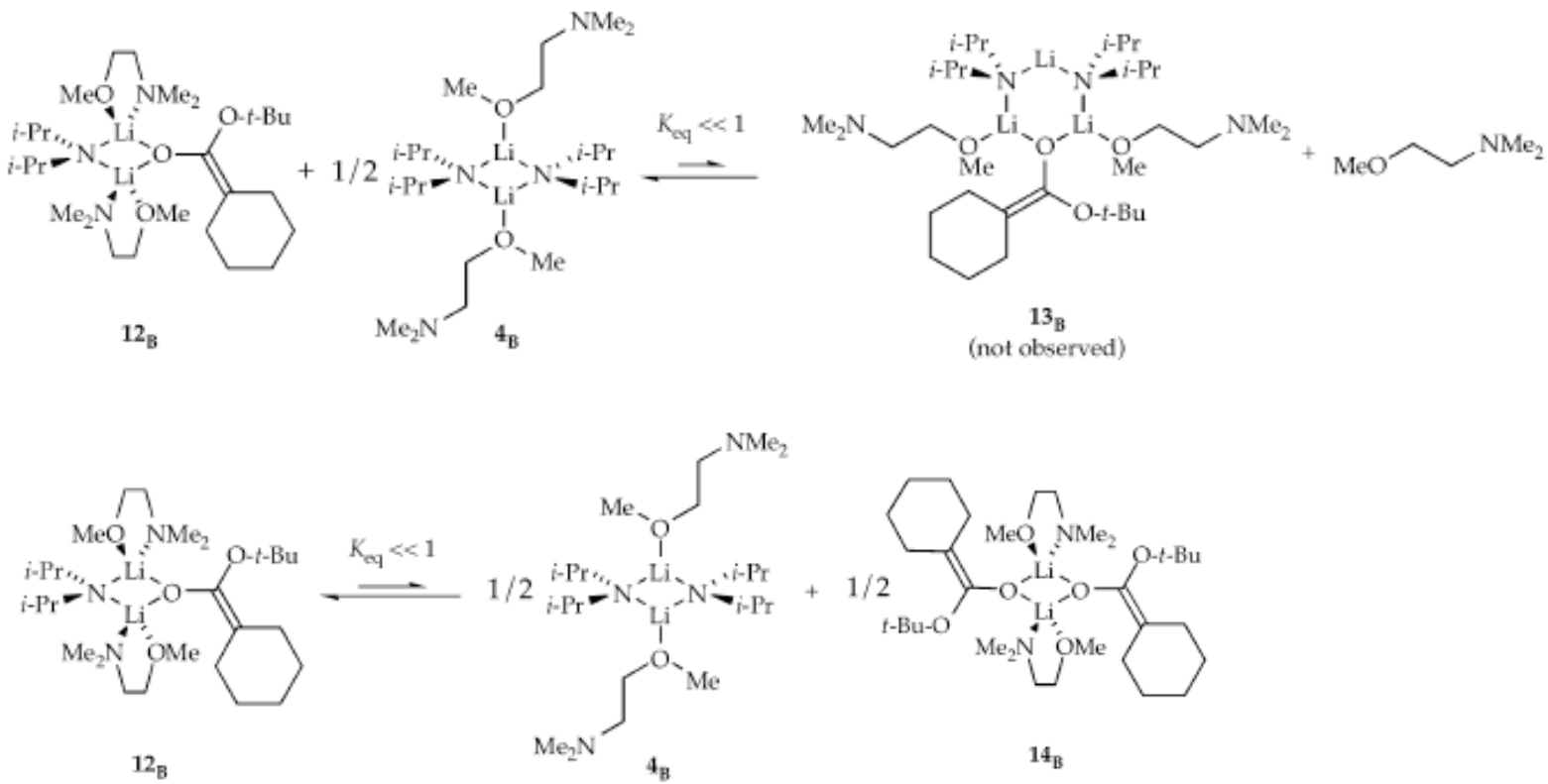


Collum, D. *et.al*. *JACS* **2006**, 128, 10326

# Summary of Enolization:

A) Enolizations of the ester by 1.0 equiv. of LDA stall at 50% Conversion due to mixed aggregates

B) Amino-ether **B** forms stable chelates of mixed dimer **12B** relative to mixed trimer as well as the homoaggregates.

C) Hindered amino-ether **C** does not chelate to LDA homodimer **4c** or mixed dimer **12c** but strongly binds to homoaggregated enolate

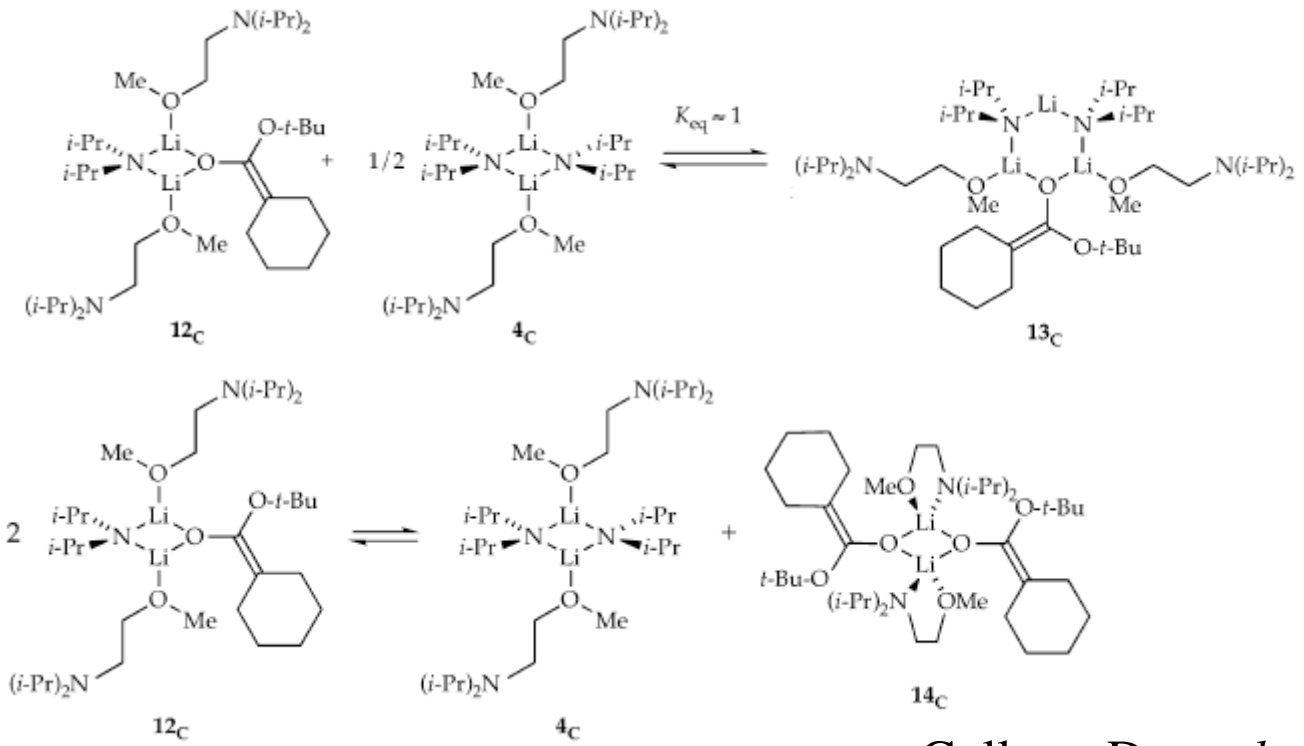


Collum, D. *et.al*. *JACS* **2006**, 128, 10326

# Mixed Dimer Derived Enolizations

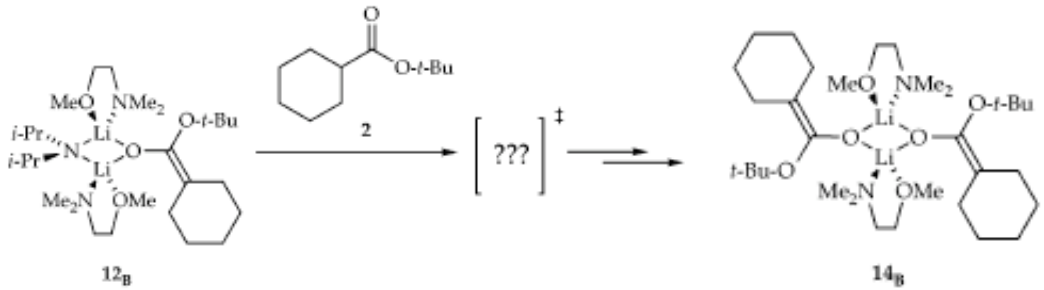


**kH / kD = 17 +/- 2**

**What are the Implications of the Rate Data on the Mechanism?**

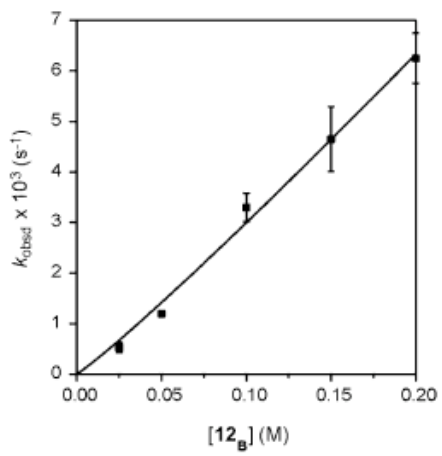


*Figure 4.* Plot of $k_{obsd}$ vs $[\mathbf{12_B}]$ in $MeOCH_2CH_2NMe_2$ (0.5 M) and hexane cosolvent for the enolization of ester **2** (0.002 M) at −60 °C. The curve depicts the result of an unweighted least-squares fit to $k_{obsd} = k\,[\mathbf{12_B}]^n$ ($k = (3.6 \pm 0.5) \times 10^{-2}$, $n = 1.1 \pm 0.1$.

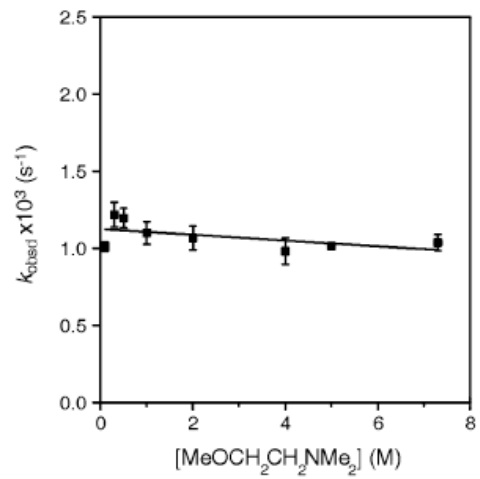


*Figure 5.* Plot of $k_{obsd}$ vs $[MeOCH_2CH_2NMe_2]$ in hexane cosolvent for the enolization of ester **2** (0.002 M) by mixed dimer $\mathbf{12_B}$ (0.05 M) at −60 °C in the presence of excess enolate $\mathbf{14_B}$ (0.005 M). The curve depicts an unweighted least- squares fit to $k_{obsd} = k\,[MeOCH_2CH_2NMe_2] + k'$ ($k = (-1 \pm 1) \times 10^{-5}$, $k' = (1.1 \pm 0.1) \times 10^{-3}$).

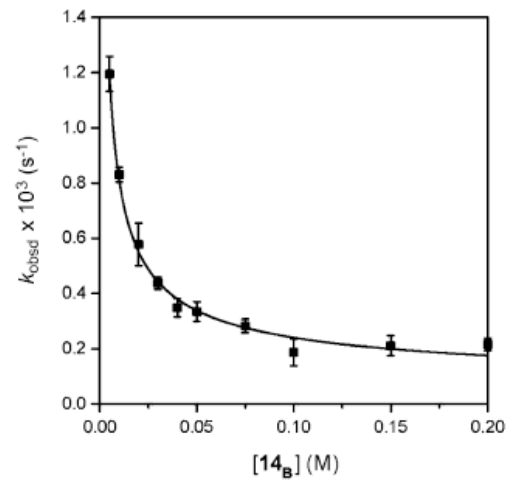


*Figure 3.* Plot of $k_{obsd}$ vs $[\mathbf{14_B}]^{22}$ in $MeOCH_2CH_2NMe_2$ (0.5 M) and hexane cosolvent for the enolization of ester **2** (0.002 M) by mixed dimer $\mathbf{12_B}$ (0.05 M) at −60 °C. The curve depicts the result of an unweighted least-squares fit to $k_{obsd} = k\,[\mathbf{14_B}]^n + k'$ ($k = (5 \pm 2) \times 10^{-5}$, $n = -0.61 \pm 0.07$, $k' = (5 \pm 5) \times 10^{-5}$).

Collum, D. *et.al*. *JACS* **2006**, 128, 10326

# Mixed Dimer Derived Enolizations

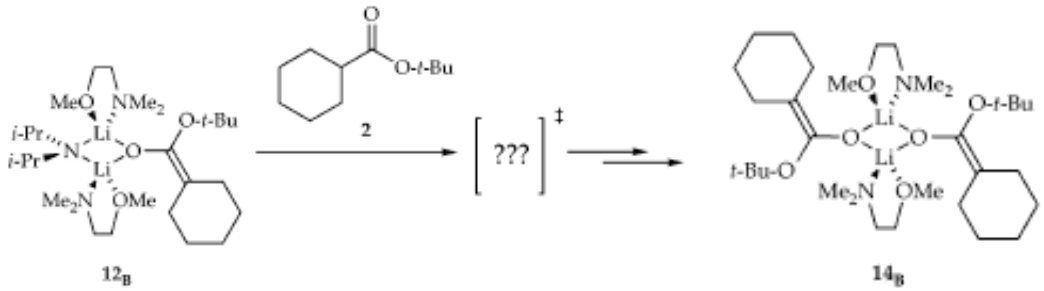


-d[**2**] / dt = *k'* [**B**]$^0$ [**12**$_B$] [ester] .....

**kH / kD = 17 +/- 2**

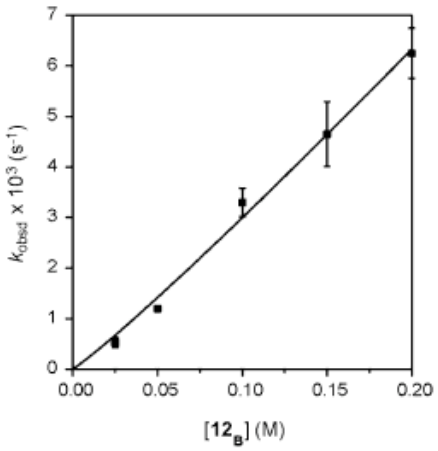


***Figure 4.*** Plot of $k_{obsd}$ vs [$\mathbf{12_B}$] in $MeOCH_2CH_2NMe_2$ (0.5 M) and hexane cosolvent for the enolization of ester **2** (0.002 M) at −60 °C. The curve depicts the result of an unweighted least-squares fit to $k_{obsd} = k\,[\mathbf{12_B}]^n$ ($k = (3.6 \pm 0.5) \times 10^{-2}$, $n = 1.1 \pm 0.1$.

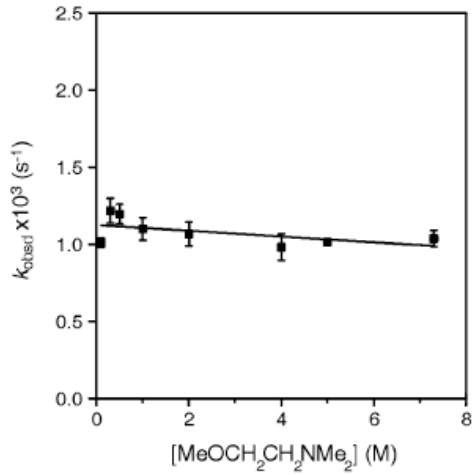


***Figure 5.*** Plot of $k_{obsd}$ vs [$MeOCH_2CH_2NMe_2$] in hexane cosolvent for the enolization of ester **2** (0.002 M) by mixed dimer $\mathbf{12_B}$ (0.05 M) at −60 °C in the presence of excess enolate $\mathbf{14_B}$ (0.005 M). The curve depicts an unweighted least- squares fit to $k_{obsd} = k\,[MeOCH_2CH_2NMe_2] + k'$ ($k = (-1 \pm 1) \times 10^{-5}$, $k' = (1.1 \pm 0.1) \times 10^{-3}$).

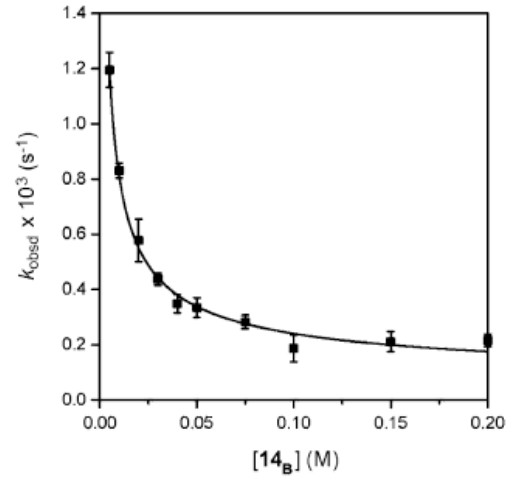


***Figure 3.*** Plot of $k_{obsd}$ vs $[\mathbf{14_B}]^{22}$ in $MeOCH_2CH_2NMe_2$ (0.5 M) and hexane cosolvent for the enolization of ester **2** (0.002 M) by mixed dimer $\mathbf{12_B}$ (0.05 M) at −60 °C. The curve depicts the result of an unweighted least-squares fit to $k_{obsd} = k\,[\mathbf{14_B}]^n + k'$ ($k = (5 \pm 2) \times 10^{-5}$, $n = -0.61 \pm 0.07$, $k' = (5 \pm 5) \times 10^{-5}$).

Collum, D. *et.al*. *JACS* **2006**, 128, 10326

# Mixed Dimer Derived Enolizations

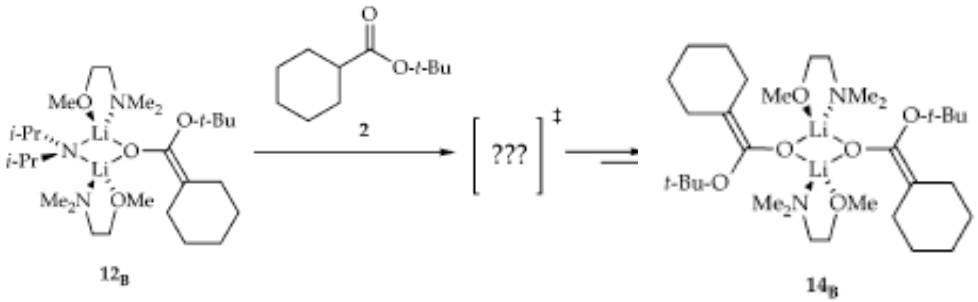


$$-d[\mathbf{2}]/dt = k'\,[\mathbf{B}]^0\,[\mathbf{12_B}]\,[\text{ester}]\,\{[\text{enolate}]^{-1/2} + [\text{enolate}]^0\}$$

**kH / kD = 17 +/- 2**

**Monomer based enolization:**

$(i\text{-Pr}_2\text{NLi})(\text{enolate})(\mathbf{B})_2 + \mathbf{2} \rightleftharpoons (i\text{-Pr}_2\text{NLi})(\mathbf{B})(\mathbf{2}) + 1/2\ (\text{enolate})_2(\mathbf{B})_2$

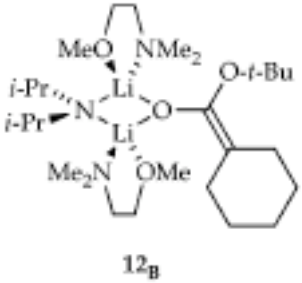


enolate

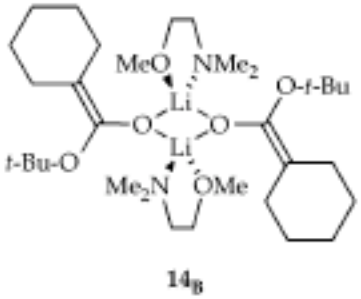


**Mixed Dimer based enolization:**

$(i\text{-Pr}_2\text{NLi})(\text{enolate})(\mathbf{B})_2 + \mathbf{2} \rightleftharpoons (i\text{-Pr}_2\text{NLi})(\text{enolate})(\mathbf{B})_2\ (\mathbf{2})$

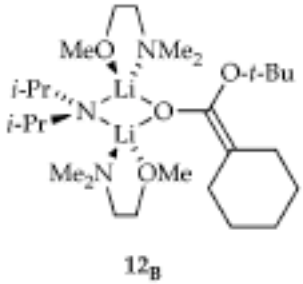


enolate

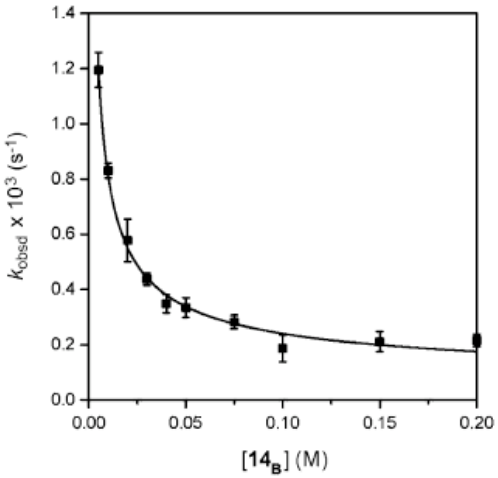


*Figure 3.* Plot of $k_{obsd}$ vs $[\mathbf{14_B}]$[22] in $MeOCH_2CH_2NMe_2$ (0.5 M) and hexane cosolvent for the enolization of ester **2** (0.002 M) by mixed dimer $\mathbf{12_B}$ (0.05 M) at −60 °C. The curve depicts the result of an unweighted least-squares fit to $k_{obsd} = k\,[\mathbf{14_B}]^n + k'$ ($k = (5 \pm 2) \times 10^{-5}$, $n = -0.61 \pm 0.07$, $k' = (5 \pm 5) \times 10^{-5}$).

Collum, D. *et.al*. *JACS* **2006**, 128, 10326

# Mixed Dimer Derived Enolizations

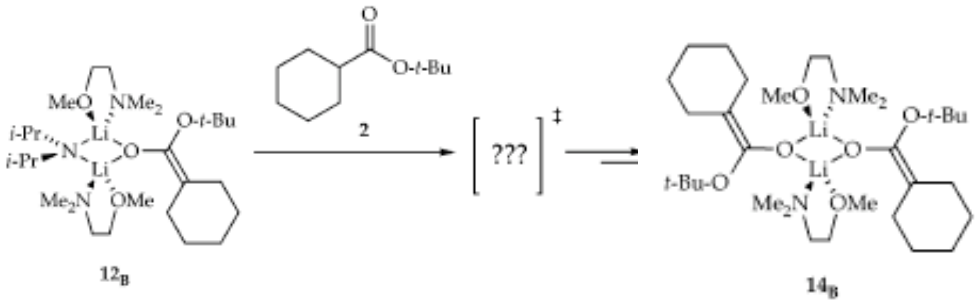


$$-d[\mathbf{2}] / dt = k' [\mathbf{B}]^0 [\mathbf{12}_B] [\text{ester}] \{ [\text{enolate}]^{-1/2} + [\text{enolate}]^0 \}$$

**kH / kD = 17 +/- 2**

**Monomer based enolization:**

($i$-$Pr_2NLi$)(enolate)($\mathbf{B}$)$_2$ + **2** $\rightleftharpoons$ ($i$-$Pr_2NLi$)($\mathbf{B}$)(**2**) + (enolate)$_2$($\mathbf{B}$)$_2$

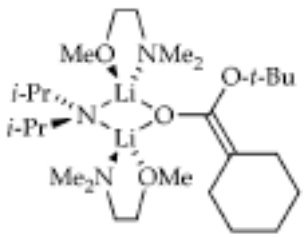


enolate

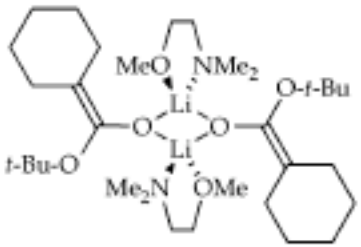


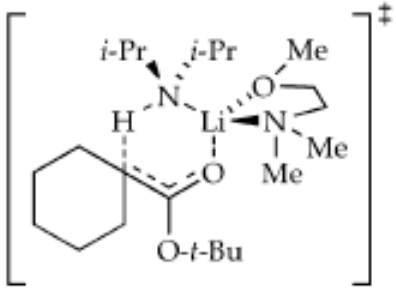


**Mixed Dimer based enolization:**

($i$-$Pr_2NLi$)(enolate)($\mathbf{B}$)$_2$ + **2** $\rightleftharpoons$ ($i$-$Pr_2NLi$)(enolate)($\mathbf{B}$)$_2$ (**2**)

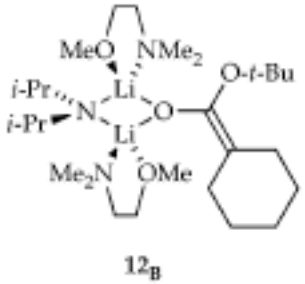


enolate

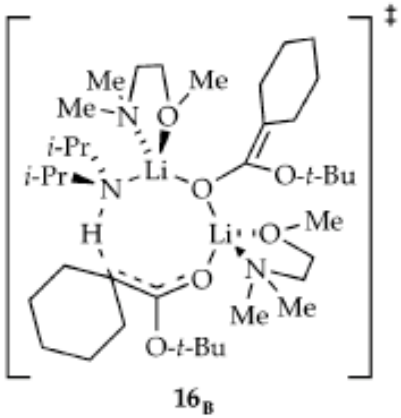


Collum, D. *et.al*. *JACS* **2006**, 128, 10326

# Mixed Dimer Derived Enolizations Summary:

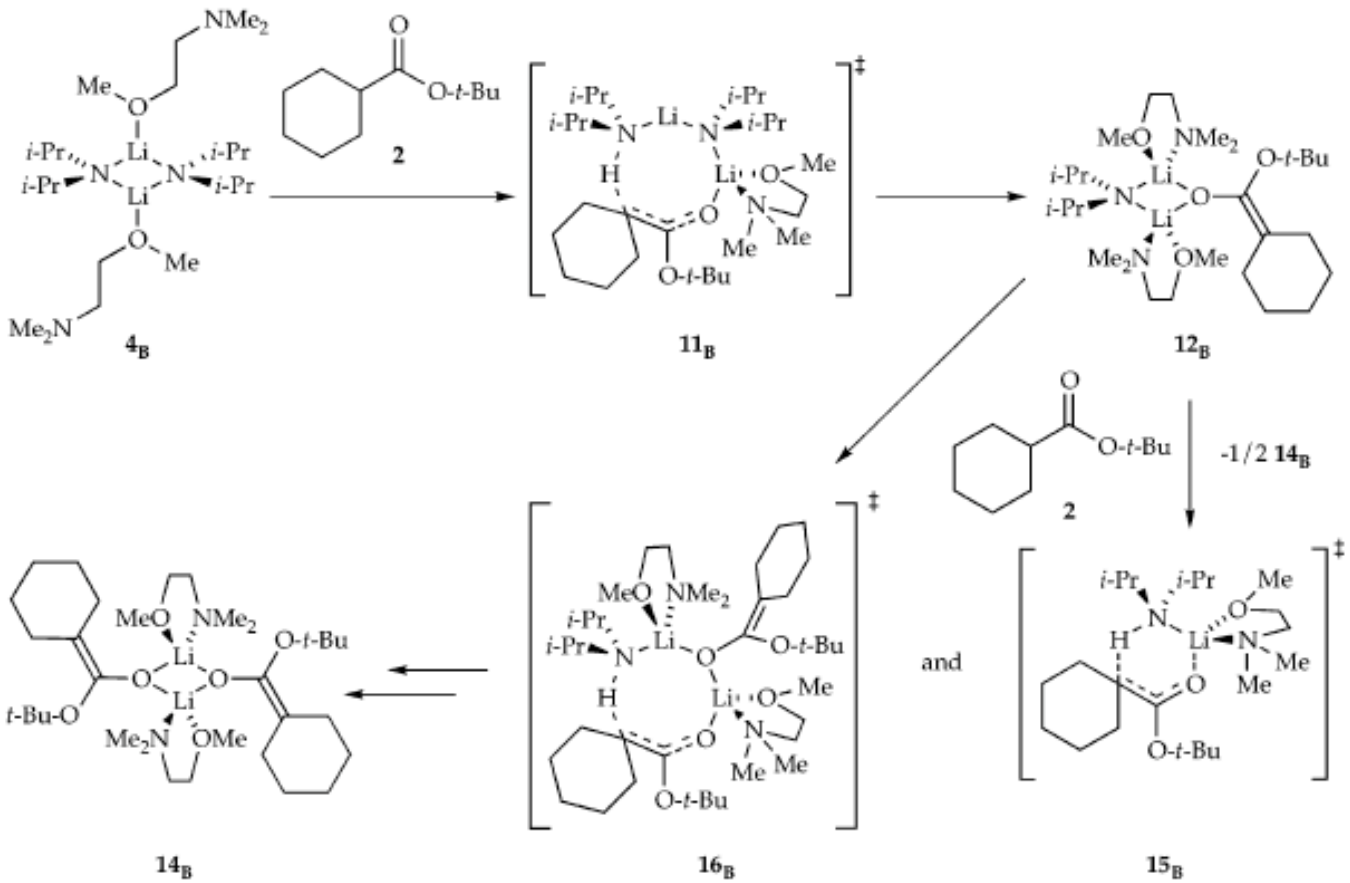


Collum, D. *et.al*. *JACS* **2006**, 128, 10326

# Ligand Catalyzed Enolization

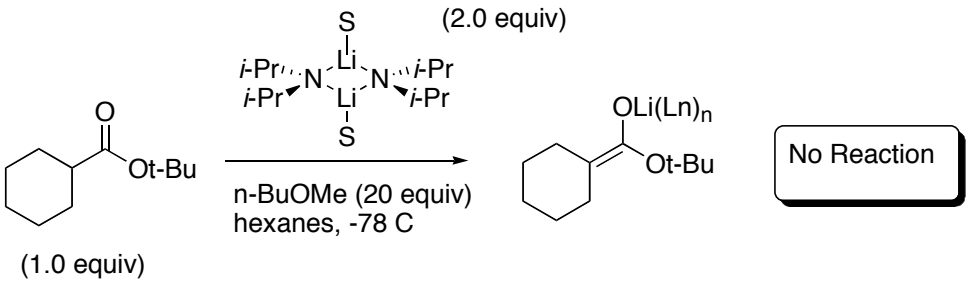


Collum, D. *et.al*. *JACS* **2006**, 128, 10326

# Ligand Catalyzed Enolization

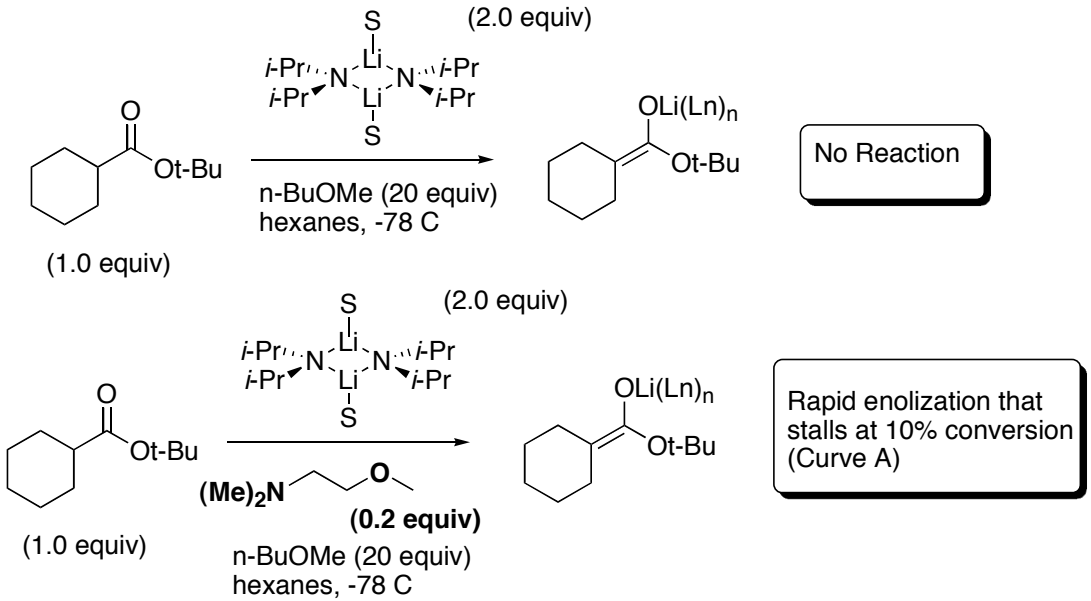


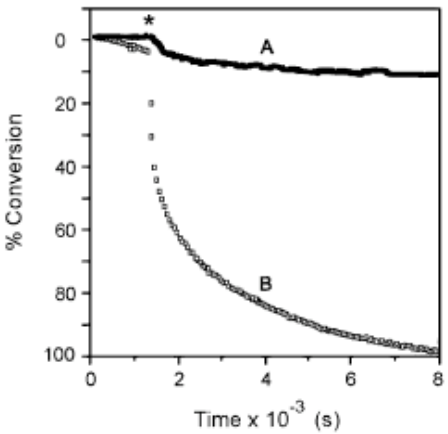


*Figure 6.* Plot of the percent conversion for the enolization of ester **2** (0.05 M) by LDA (0.1 M) at −78 °C in hexane containing: (A, ■) *n*-BuOMe (1.0 M); (B, □) $MeOCH_2CH_2N(i\text{-}Pr)_2$ (1.0 M). The asterisk indicates the addition of 0.2 equiv of ligand **B** relative to ester **2**.

Collum, D. *et.al*. *JACS* **2006**, 128, 10326

# Ligand Catalyzed Enolization

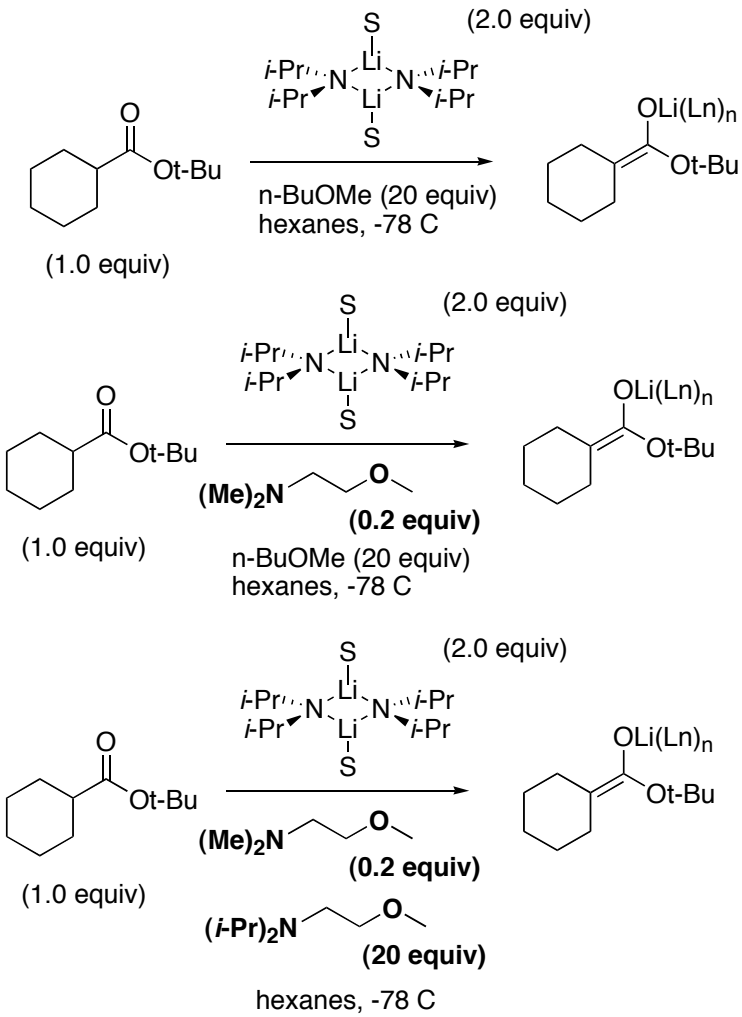


No Reaction

Rapid enolization that stalls at 10% conversion (Curve A)

Enolization goes to >95% completion

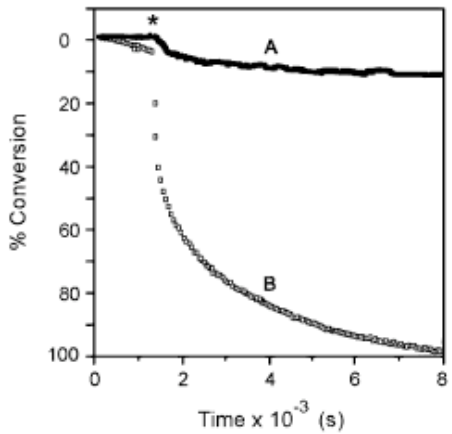


*Figure 6.* Plot of the percent conversion for the enolization of ester **2** (0.05 M) by LDA (0.1 M) at −78 °C in hexane containing: (A, ■) *n*-BuOMe (1.0 M); (B, □) $MeOCH_2CH_2N(i\text{-}Pr)_2$ (1.0 M). The asterisk indicates the addition of 0.2 equiv of ligand **B** relative to ester **2**.

Collum, D. *et.al*. *JACS* **2006**, 128, 10326

# Ligand Catalyzed Enolization

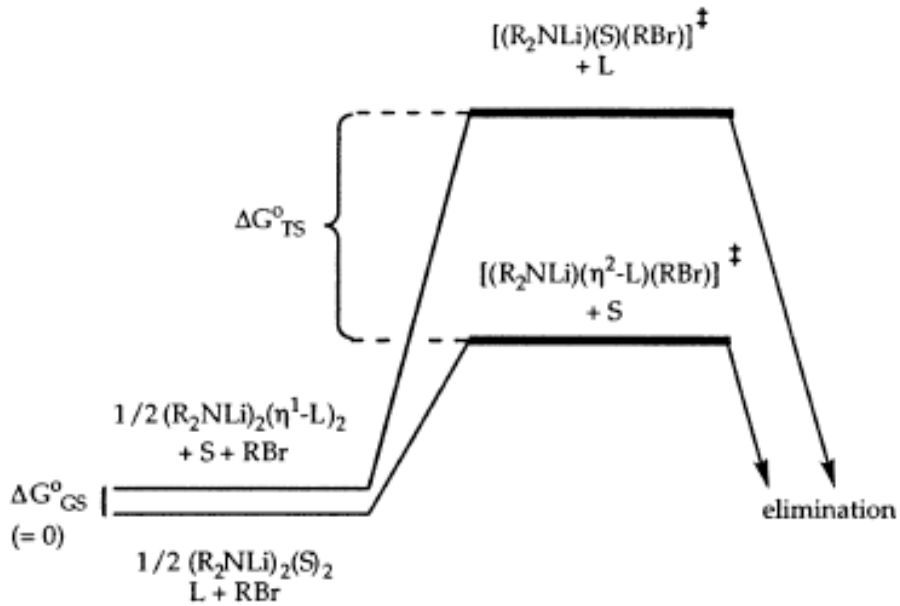


Ligand **C** facilitates dissociation of **B** by coordinating homoenolate dimer **14**. This shifts the mixed aggregate - homoaggregate equillibira to allow turnover.

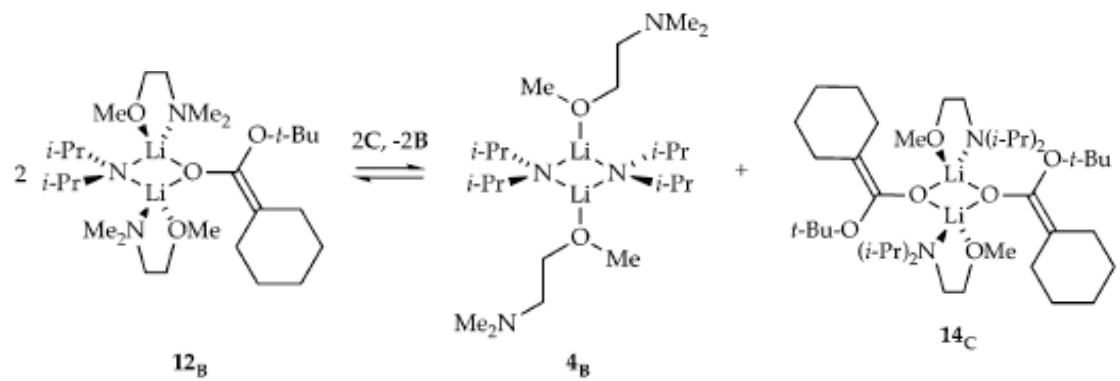


Collum, D. *et.al*. *JACS* **2006**, 128, 10326

# Summary:

-Between 1985 and 2002 at the Pfizer-Groten site 68.4% of all C-C bond forming reactions were carbanion based (aldol, enolate alkylation, Micheal additions, enolate additions to imine / ketimine, lithium carbanion addition, ect….).

-The structural and mechanistic complexity of these reactions does not preclude their detailed study. Though, it should be noted that it is because of this complexity that "..a vast number of organolithium reagents are routinely generated and used without direct evidence of their solution structures, dynamic behavior, or even existence." (Collum, D. *Acc. Chem. Res.* **1993**, 26, 227.)

-"I believe that, for those who seek to discover new reactions, the most insightful lessons come from trying to trace important reactivity principles back to their origns." (Sharpless, B. *Proc. Robert A. Welch foundation Conf. Chem. Res.* **1984**, 27, 59.)

Dugger, R. *et. al. Org. Process Res. Dev.* **2005**, 9, 253.
Collum, D. *et. al. Angew. Chem. Int. Ed.* In Press.

# Title

# Substituent Effects on Lithium Ion Coordination:

Is there a *gem*-dimethyl effect on lithium ion chelation?

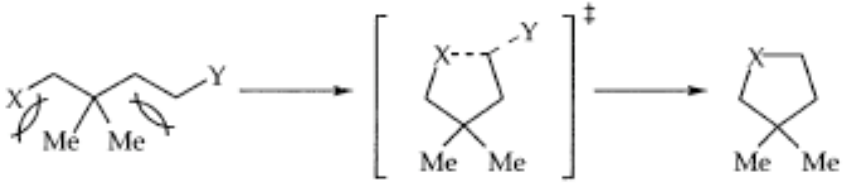


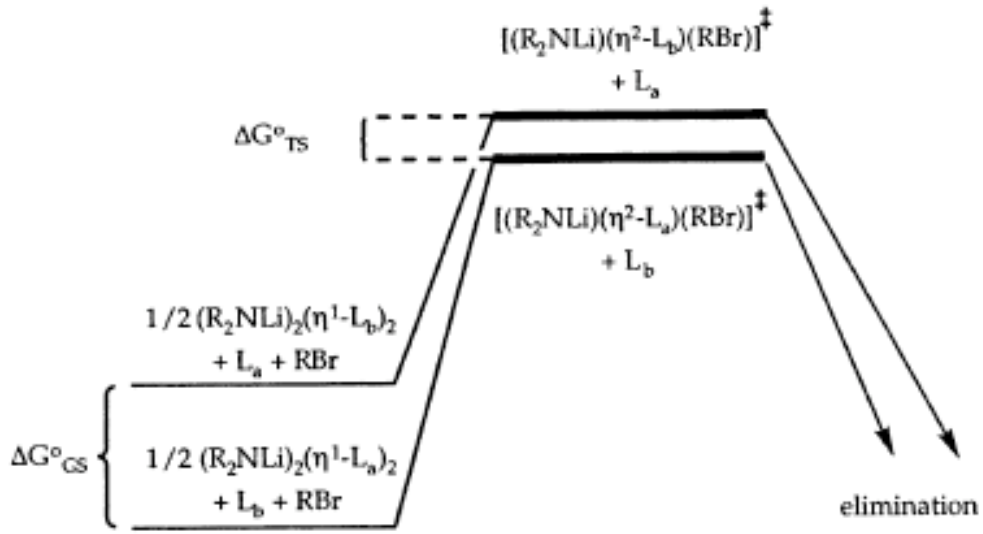


Collum, D. *et.al*. *JACS* **2003**, 125, 15376.

# Substituent Effects on Lithium Ion Coordination:

Is there a *gem*-dimethyl effect on lithium ion chelation?

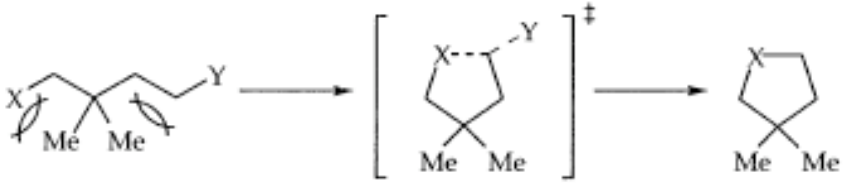


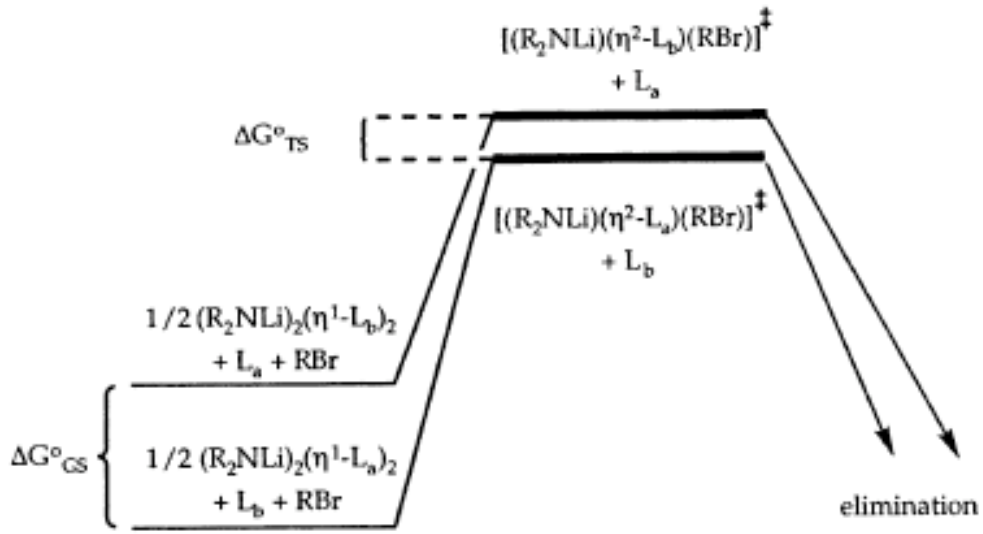


## Model Reaction:

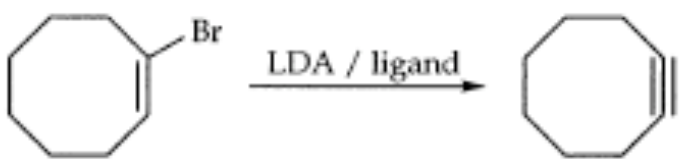


**1** **2**

**Clean first order behavior in [1]**
**Significant KIE's show proton abstraction as the rate-limiting**

**LDA Order = 0.5**
**Ligand Order = 0**

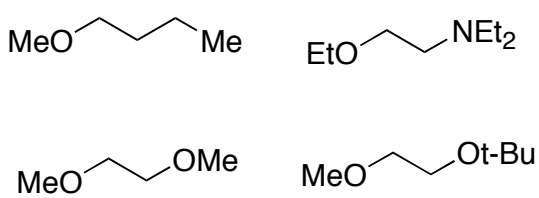


$$-d[1]/dt = k'[1]^1[LDA]^{1/2}[n\text{-BuOMe}]^0 \quad (4)$$

$$^1/_2(i\text{-Pr}_2\text{NLi})_2(n\text{-BuOMe})_2 \rightleftharpoons (i\text{-Pr}_2\text{NLi})(n\text{-BuOMe}) \quad (5)$$

$$(i\text{-Pr}_2\text{NLi})(n\text{-BuOMe}) + 1 \rightarrow [(i\text{-Pr}_2\text{NLi})(n\text{-BuOMe})(1)]^{\ddagger} \quad (6)$$

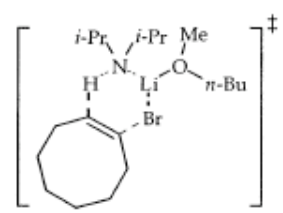


**4**

Collum, D. *et.al*. *JACS* **2003**, 125, 15376.

# Is there a *gem*-dimethyl effect?

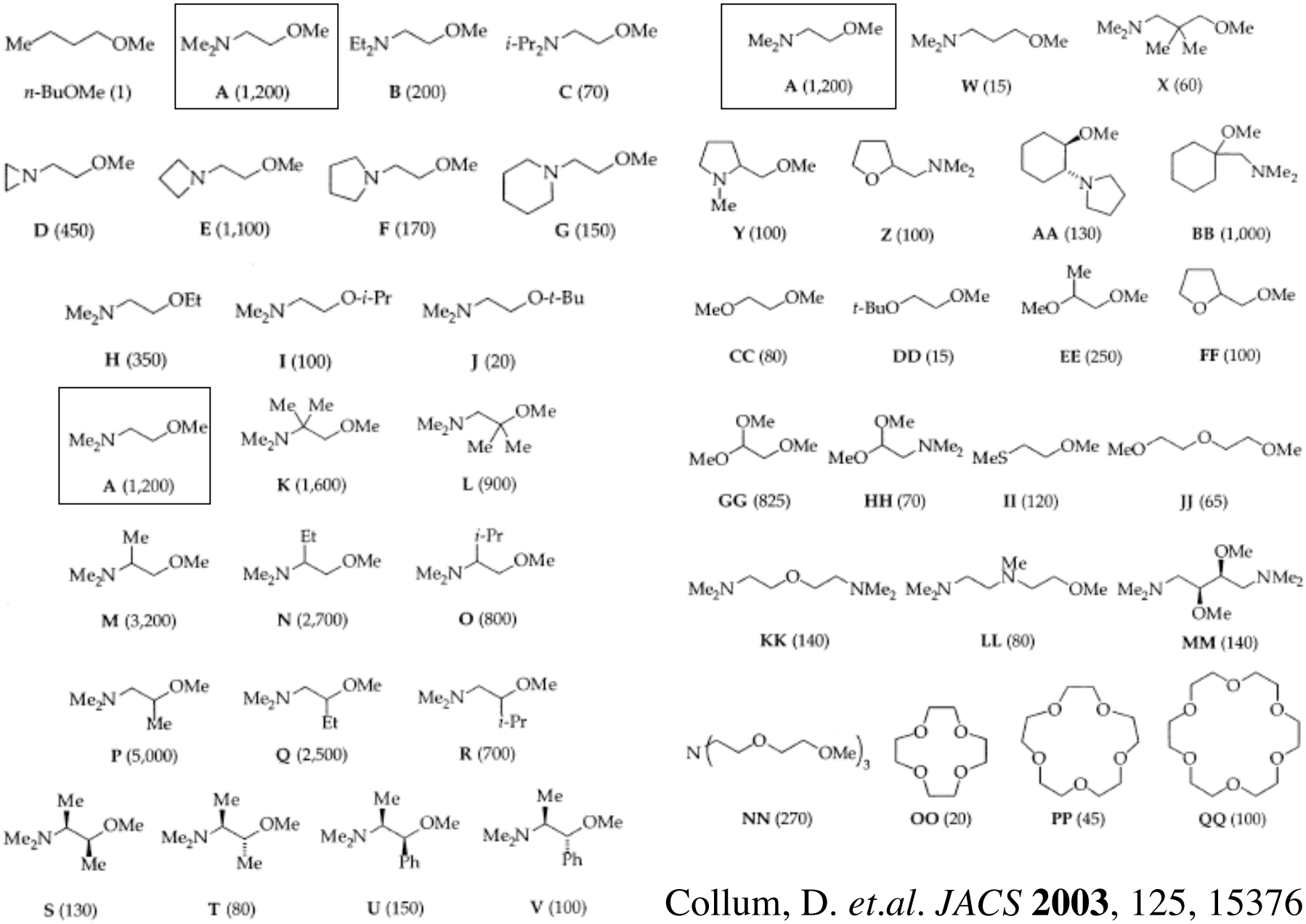


Collum, D. *et.al*. *JACS* **2003**, 125, 15376.

# Thermochemical analysis of Hemilibility

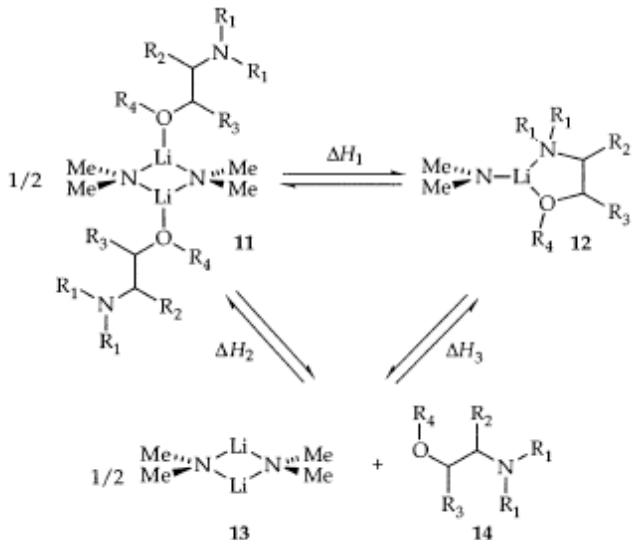


*Table 3.* Calculated Enthalpies (kcal/mol) of Monomer Aggregation ($\Delta H_1$), Dimer Solvation ($\Delta H_2$), and Monomer Solvation ($\Delta H_3$) for $Me_2NLi$ Coordinated to Ligands Substituted on the Two-Carbon Backbone[a]

| ligand | $\Delta H_{f(Ligand)}$ | $\Delta H_1$ | $\Delta H_2$ | $\Delta H_3$ |
|---|---|---|---|---|
| **K** | −35.0 | 8.7 | −5.1 | 3.6 |
| **L** | −38.9 | 8.2 | −5.1 | 3.1 |
| **M** | −43.3 | 9.1 | −5.6 | 3.5 |
| **N** | −46.9 | 8.2 | −3.4 | 4.8 |
| **O** | −44.2 | 8.5 | −3.0 | 5.5 |
| **P** | −44.4 | 8.5 | −5.0 | 3.5 |
| **Q** | −47.5 | 6.9 | −3.0 | 3.9 |
| **R** | −47.1 | 7.2 | −2.1 | 5.1 |
| **S** | −41.9 | 6.8 | −2.7 | 4.1 |
| **T** | −42.3 | 9.0 | −4.0 | 5.0 |
| **U** | −8.0 | 7.4 | −3.3 | 4.1 |
| **V** | −8.3 | 10.6 | −5.9 | 5.5 |
| av dev[b] | – | 1.1 | 1.3 | 0.8 |

[a] The average deviation of the enthalpies is represented by. The heats of formation (kcal/mol) of ligands **K**−**V** in their most stable conformations is represented by $\Delta H_{f(Ligand)}$. $(Me_2NLi)_2 = -60.5$ kcal/mol. [b] Av dev = average deviation.

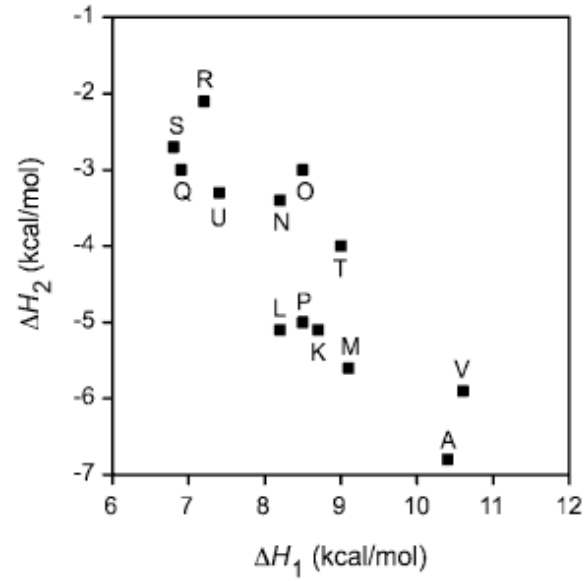


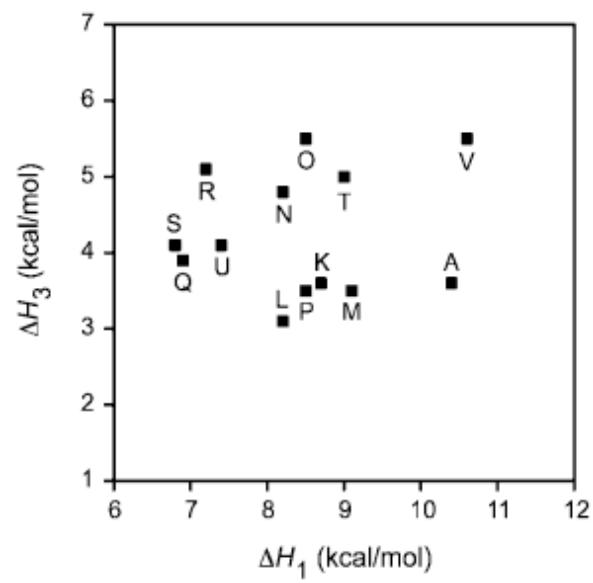


Collum, D. *et.al*. *JACS* **2003**, 125, 15376

# Computational Vs. Free Energies

A comparison of computational methods Vs. the free energies
Of activation